Effects of Clouds, Soil Moisture, Precipitation, and Water Vapor on Diurnal Temperature Range

AIGUO DAI AND KEVIN E. TRENBERTH

National Center for Atmospheric Research, Boulder, Colorado*

THOMAS R. KARL

NOAA/National Climatic Data Center, Asheville, North Carolina

(Manuscript received 9 July 1998, in final form 9 September 1998)

ABSTRACT

The diurnal range of surface air temperature (DTR) has decreased worldwide during the last 4–5 decades and changes in cloud cover are often cited as one of the likely causes. To determine how clouds and moisture affect DTR physically on daily bases, the authors analyze the 30-min averaged data of surface meteorological variables and energy fluxes from the the First International Satellite Land Surface Climatology Project Field Experiment and the synoptic weather reports of 1980–1991 from about 6500 stations worldwide. The statistical relationships are also examined more thoroughly in the historical monthly records of DTR, cloud cover, precipitation, and streamflow of this century.

It is found that clouds, combined with secondary damping effects from soil moisture and precipitation, can reduce DTR by 25%–50% compared with clear-sky days over most land areas; while atmospheric water vapor increases both nighttime and daytime temperatures and has small effects on DTR. Clouds, which largely determine the geographic patterns of DTR, greatly reduce DTR by sharply decreasing surface solar radiation while soil moisture decreases DTR by increasing daytime surface evaporative cooling. Clouds with low bases are most efficient in reducing the daytime maximum temperature and DTR mainly because they are very effective in reflecting the sunlight, while middle and high clouds have only moderate damping effects on DTR. The DTR reduction by clouds is largest in warm and dry seasons such as autumn over northern midlatitudes when latent heat release is limited by the soil moisture content. The net effects of clouds on the nighttime minimum temperature is small except in the winter high latitudes where the greenhouse warming effect of clouds exceeds their solar cooling effect.

The historical records of DTR of the twentieth century covary inversely with cloud cover and precipitation on interannual to multidecadal timescales over the United States, Australia, midlatitude Canada, and former U.S.S.R., and up to 80% of the DTR variance can be explained by the cloud and precipitation records. Given the strong damping effect of clouds on the daytime maximum temperature and DTR, the well-established worldwide asymmetric trends of the daytime and nighttime temperatures and the DTR decreases during the last 4–5 decades are consistent with the reported increasing trends in cloud cover and precipitation over many land areas and support the notion that the hydrologic cycle has intensified.

1. Introduction

The diurnal range of surface air temperature (DTR) has decreased since the 1950s worldwide (especially over the Northern Hemisphere land areas) mainly but not always due to an increase in nighttime minimum temperature (T_{min}) that exceeds the increase in daytime maximum temperature (T_{max}) (Karl et al. 1993; Horton 1995; Houghton et al. 1996; Easterling et al. 1997). Coincident increases in total cloud cover have been found in a number of locations (Henderson-Sellers 1992; Dessens and Bücher 1995; Kaas and Frich 1995; Jones 1995) and are often cited as a likely cause for the observed DTR decrease (Kukla and Karl 1993; Karl et al. 1993; Karl et al. 1996; Dai et al. 1997a). Annual and seasonal DTR are strongly correlated with cloud cover over the contiguous United States with the highest correlation in autumn (Plantico and Karl 1990; Karl et al. 1993). A jump in cloud cover was found to concur with a large decrease in DTR over the former U.S.S.R. (Karl et al. 1996). Strong correlation between annual DTR and cloud cover/precipitation also exists over other continents where data are available (Dai et al. 1997a).

Clouds can reduce T_{max} by reflecting the sunlight and

* The National Center for Atmospheric Research is sponsored by the National Science Foundation.

Corresponding author address: Dr. A. Dai, NCAR, P.O. Box 3000, Boulder, CO 80307.
E-mail: adai@ucar.edu

increase T_{min} by enhancing downward longwave radiation. A global climate model (GCM) study (Hansen et al. 1995) suggests that clouds at all levels can reduce DTR, although water vapor feedback may limit the damping effects of low-level clouds on DTR. GCM experiments (Cao et al. 1992; Mitchell et al. 1995) show that the largest DTR reduction in increased CO_2 climates is associated with large increases in cloud cover, soil moisture (where evaporation is restricted by the soil moisture content), and snow cover. However, little correlation exists between winter snow cover and DTR at many U.S. stations (Karl et al. 1993). Soil moisture can damp DTR through evaporative cooling, which is effective during the day when the planetary boundary layer is unstable and the potential evapotranspiration is high. We therefore expect larger evaporative cooling effect on T_{max} rather than T_{min}, especially during the dry and warm seasons. A radiative–convective model study (Stenchikov and Robock 1995) suggests that (a) infrared radiative forcings mainly affect the daily mean temperature while solar forcings directly modulate DTR, (b) water vapor reduces DTR due to its absorption of the solar radiation in the near infrared, and (c) combined with a 50% CO_2 increase, tropospheric aerosol pollution decreases DTR.

Clouds, soil moisture, and water vapor are largely local forcings on DTR. Surface air temperatures can also be changed rapidly by the passing of synoptic systems. In general, however, synoptic systems are random and the frontal advection of cold or warm air itself affects surface air temperatures on $\geq$24-h timescales. This should have small effects on the time-averaged DTR. On the other hand, the airmasses separated by a front may have very different humidity and cloudiness (e.g., rainy days tend to be associated with frontal passages in winter and spring in midlatitudes), which could potentially result in different DTR. Diurnal variations in surface wind direction (such as sea breezes) may also affect DTR through advection of air mass with different temperatures and humidity.

Previous observational studies on the effects of clouds and precipitation on DTR (e.g., Karl et al. 1993; Karl et al. 1996; Dai et al. 1997a; Campbell and Vonder Haar 1997; Power et al. 1998) used only monthly or annual data and focused mostly on the correlative relationships on interannual to decadal timescales. In this study, we analyzed hourly and daily station data of surface air temperatures, humidity, cloud cover, precipitation, soil moisture, and winds to quantify the effects of these hydrological variables and winds on DTR. By stratifying the data (e.g., clear versus cloudy days, low humidity versus high humidity days, etc.), we are able to isolate, to a large extent, the effect of each of the variables on DTR, thereby identifying the major variables or processes that control DTR. To more firmly establish the physical basis for the statistical results, we examined the main terms in the surface energy budget using the high-resolution data from the First International Satellite Land Surface Climatology Project (ISLSP) Field Experiment (FIFE). We also examine the long-term DTR-clouds–precipitation relationships using monthly data of this century. Our results provide more evidence of the strong damping effects of clouds on DTR.

The results presented in this paper include those from correlative and composite analyses of daily data from FIFE and global weather stations, and those from the correlative and regression analyses of the historical monthly data for the twentieth century. The correlative and composite analyses of the daily data complement each other and point to similar conclusions, which provide the physical basis for the statistical relationships found in the historical records. In section 2 we describe the datasets and the analysis procedures used in this study. The results from analyses of daily and monthly data are presented in section 3, in which we first describe the correlative and composite results from the FIFE data, those from the global station data, and the statistical results from the historical data of the twentieth century. In section 4 we summarize the results and discuss the implications.

2. Data and analysis procedures

From May 1987 to late 1989 an extensive series of surface data were collected at a 15 km $\times$ 15 km site centered at (39.05°N, 96.53°W) over the Konza prairie near Manhattan, Kansas, during the First International Satellite Land Surface Climatology Project (ISLSP) Field Experiment. Based on the high-resolution data collected at about 10 stations and from other sources, Betts and Ball (1998) created a FIFE site-average dataset (referred to as the FIFE dataset in this paper). The FIFE dataset contains, among other things, 30-min averaged values of surface air temperature, humidity, winds, precipitation, total cloud cover, latent and sensible heat fluxes, solar and longwave radiative fluxes, and daily values of soil moisture content. Since cloud cover data are incomplete in the FIFE dataset, we extracted cloud cover reports at a nearby weather station (WMO station ID: FRI, location: 39.05°N, 96.77°W), from the National Center for Atmospheric Research (NCAR) Data Archives (DS464.0, http://www.scd.ucar.edu/dss/datasets/ds464.0.html) to complement the FIFE dataset (the two records of cloud cover have a correlation coefficient of 0.87 during their overlapped days). The high temporal resolution and the complete heat and radiative fluxes of the FIFE dataset enable us to analyze the diurnal cycle of surface air temperature and the energy terms that drive the diurnal variations. As the FIFE data are insufficient for spring and winter seasons (few field measurements were made in the cold seasons), we will focus on summer and autumn results.

We first performed a correlative analysis of the daily DTR, cloud cover, surface humidity, precipitation, surface wind speed, and soil moisture content using the

FIFE dataset. Both the simple and partial correlations (i.e., after removing the effects of the other variables, see, e.g., Hair et al. 1987) between the DTR and the other variables were calculated and examined for their possible effects on or association with DTR. Cross correlations among these state variables were also examined for the interdependence among them. The correlative relationships between the surface energy fluxes and the above state variables were also analyzed. The analysis was stratified by season.

The correlative analysis provides only statistical associations between DTR and other variables. To examine how winds, clouds, humidity, soil moisture, and precipitation affect the surface energy fluxes and thus DTR and to isolate, to a large extent, the individual effect of these variables on DTR, we stratify the FIFE data into six cases described below and compare the mean DTR and heat and radiative fluxes between the two categories of days within each case. In each case, the state variables (cloud cover, surface humidity, wind direction, and daily mean soil moisture content) are examined and usually there is only one state variable with significant differences between the two compared categories. Therefore, most of the differences between the DTR of the two categories can be traced back to a particular forcing for each case.

Case 1 (effects of wind direction): Choose relatively clear (daily mean cloud cover cc $\leq$25%) days, separate them into two categories of days with northerly (daily mean meridional wind component $v < 0$) and southerly ($v > 0$) winds. The predominant winds come from the south to southwest and less frequently from the west to northwest at the FIFE site during summer and autumn. This case is designed to highlight the effect of the advection of warm and cool air masses on surface air temperatures and DTR. The number of the sampled days with northerly (southerly) winds is 6 (49) for summer and 20 (47) for autumn.

Case 2 (effects of clouds): choose nonprecipitating ($<$1 mm day^{-1}) and relatively dry (top 5-cm soil moisture content sm $<$23.2% by volume or the 50th percentile) days, separate them into clear (cc $\leq$ 12.5% or one okta) and cloudy (cc $\geq$ 62.5% or five oktas) days. By excluding the precipitating days and the wet-ground days, the effects of soil moisture and precipitation on DTR are minimized. The number of the clear (cloudy) days is 19 (16) for summer and 13 (7) for autumn.

Case 3 (effects of water vapor): choose relatively clear and dry days with cc $\leq$25% and sm $<$23.2%, separate them into low humidity [daily mean surface specific humidity $q < 11.0$ g kg^{-1} in summer (June–August or JJA) and $q < 6.0$ g kg^{-1} in autumn (September–November or SON)] and high humidity ($q > 14.5$ g kg^{-1} for JJA and $q > 9.7$ g kg^{-1} for SON) categories. Ideally, atmospheric precipitable water should be used here. Unfortunately, there are insufficient radiosonde data to derive atmospheric precipitable water with a diurnal cycle for the FIFE site. Nevertheless, there are large differences in the downward longwave radiation at the surface between the low and high surface humidity days. This suggests that for our purpose (i.e., to examine the effect of water vapor on DTR through its downward longwave radiation) the use of surface humidity is sufficient. The number of the low (high) humidity days is 8 (9) for summer and 9 (6) for autumn.

Case 4 (effects of soil moisture): Choose relatively clear days (cc $\leq$ 25%), separate them into low (sm $<$ 19.0%) and high (sm $>$ 25.4%) soil moisture categories. The data were not further stratified here by surface wind speed because, as we show below, wind speed has small effects on DTR at the FIFE site. The number of the low (high) sm days is 19 (13) for summer and 14 (13) for autumn.

Case 5 (effects of surface wind speed): Choose relatively clear days (cc $\leq$ 25%), separate them into calm (wind speed $V < 2.7$ m s^{-1}) and windy ($V > 4.6$ m s^{-1} for JJA and $V > 4.0$ m s^{-1} for SON) days. This case is designed to show whether surface wind speed affects the latent and sensible heat fluxes and thus DTR. The number of the calm (windy) days is 24 (17) for summer and 44 (10) for autumn.

Case 6 (combined effects of clouds, soil moisture, precipitation, and others): separate all the days into clear (cc $\leq$ 12.5%) and cloudy (cc $>$ 62.5%, including precipitating days) categories based on cloud cover only. The number of the clear (cloudy) days is 27 (97) for summer and 26 (53) for autumn.

The above stratifying criteria are based on their percentiles so that the two categories contain a number ($>$5) of days comparable to each other. Also, a limited number of observations prevented us from using more discriminating criteria in some of the cases. For example, if we further exclude high humidity days in case 4, the samples would become too small to provide meaningful results. As shown below, the state variables are usually comparable between the two categories except for the variable of interest in each case.

In this paper, we will present only the diurnal evolution of downward solar and longwave radiative fluxes, and the surface latent and sensible heat fluxes. Other energy fluxes such as the net radiation, upward longwave radiation, upward solar radiation (reflection), and heat flux into the soil are available and have been analyzed but are not shown here because their diurnal curves are similar to one of the energy fluxes shown (e.g., the net radiation is very similar to the downward solar radiation), or because they are not directly related to the state variables (i.e., cloud cover, humidity, etc.) of interest, or not correlated with DTR. Preliminary checks of the internal consistency of the surface energy fluxes were carried out during the compilation of the dataset (Betts and Ball 1998). The diurnal amplitude of the downward longwave radiation is about 30–40 W m^{-2} or 10%, while the diurnal amplitude of the upward longwave radiation is about 110–130 W m^{-2} or 20%–25%, which is consistent with the magnitude of DTR.

Here we will focus on the differences between the two categories of days in each case rather than the complete energy balance at the surface.

The composite analysis described above requires that the variables of interest (i.e., cloud cover, surface humidity, soil moisture, precipitation, and winds) are not intercorrelated strongly and that the dataset is large enough for sufficient resampling. As we show below, the cross correlations among these variables are either low ($\leq$0.35) or statistically insignificant on the daily timescale. The FIFE dataset contains three summers and autumns from 1987 to 1989. It is sufficient for most of the cases with a number of sampled days between 15 and 90. For some of the variables, in a few cases, the sampled days may be only between 5 and 15, which is barely adequate. We will show the one-standard deviation error bars for each of the composite curves. They may be used to judge the significance of the differences between the two curves.

To extend the above analysis to other locations, we extracted surface station synoptic weather reports of daily maximum and minimum air temperatures (not available for Australian stations), dewpoint depression (converted to specific humidity), winds, cloud cover, cloud type, and weather conditions (precipitation or no precipitation) from the NCAR Data Archives (DS464.0), which contains eight reports per day of surface weather conditions from about 6500 meteorological stations around the world since 1976. We processed only 12 yr of data from 1980 to 1991 (each year contains about 2.6 GB of data). Our tests showed that the results are robust if four or more years of data are used. Unlike the FIFE dataset, there are no reports of soil moisture, heat, or radiative fluxes in the station dataset. Thus we can only examine correlations between DTR (derived from the station reports of $T_{\max}$ and $T_{\min}$) and cloud cover and other variables, and the ratio of DTR between the two categories of days within each case. The same cloud cover criteria (i.e., cc $\leq$ $\frac{1}{8}$ for clear days and cc $\geq$ $\frac{5}{8}$ for cloudy days) are used in the global analysis and the low and high criteria of q and V are defined as the lower and upper one-third, respectively, of their percentiles of all the relatively clear (cc $\leq$ 25%) days within each season. The calculations were done at each station and the DTR ratio and the confidence level for the DTR differences (based on Student's t-test) were gridded by first simply averaging all the stations within each 1° $\times$ 1° grid box and then interpolating them onto a 5° long $\times$ 4° lat grid for mapping.

We also computed the low, middle, and high cloud cover based on the station reports of total cloud cover, low, or middle cloud cover, cloud base height, and existence of various cloud types. The procedure for computing cloud type amount based on the station reports is discussed in detail by Hahn et al. (1996). We also used the observed cloud base height (CBH) in determining whether the observed low or middle cloud amount (Nh) is low or middle clouds (Nh is considered as low cloud cover when CBH $<$ 2 km above the ground and as middle cloud cover when CBH $\geq$ 2 km). We then investigated the effects of these cloud amounts on DTR by examining the correlation coefficients between DTR and the cloud amounts and the composite DTR ratios between clear sky days (cloud amount $\leq$1 okta) and the days with cloud amount $\geq$5 oktas.

The predominant wind directions and the associated advection of air mass vary from one station to another because of the differences in geography and topography. Therefore, it is difficult to quantify the effects of wind direction on DTR for the ~6500 stations worldwide. The FIFE data suggest that while the daily mean surface air temperature can be affected significantly by changes in wind direction, DTR depends mostly on the diurnally asymmetric local forcing such as solar and latent heat fluxes, as one might expect. Therefore, in the composite analysis of the global station data, we did not include wind direction as a stratifying variable. We recognize that over regions where diurnal changes in wind direction are large (such as sea breezes), the differences in the diurnal cycle of wind direction (and the associated advection of air mass) between the two compared categories of days may also contribute to the DTR differences between the two categories.

To investigate the relationships between DTR and cloud cover–precipitation on interannual to decadal timescales, we used the historical (1900–1995) monthly data (on a 2.5° $\times$ 2.5° global grid) of daily maximum and minimum temperatures derived from the National Oceanic and Atmospheric Administration National Climatic Data Center GHCN v2 dataset (Peterson and Vose 1997) and precipitation from Dai et al. (1997b). The continental cloud cover data are from Henderson-Sellers (1992) and Karl and Steurer (1990). We also used available streamflow data (described in Dai et al. 1998) as a proxy of regional soil moisture contents. Data for eastern China cover only the 1952–88 period. All the cloud and streamflow data end in the 1980s. The streamflow data of the U.S. start around 1930. Data for the former U.S.S.R. cover the period from the middle 1930s to middle 1980s. As discussed in the cited references, there are various sources of error in these datasets and considerable efforts have been devoted to correct them (e.g., Karl and Steurer 1990; Dai et al. 1997b). In particular, the changes in cloud observing practice and rain gauges can induce decadal to long-term changes in the area-averaged records of cloud cover and precipitation. The inhomogeneities in cloud cover data are the result, primarily, of the addition of more observations and, especially, nighttime observations per day into the recent (post the 1940s) record (Henderson-Sellers 1989). Nevertheless, the cloud cover data over the United States, Australia, and China appear to be reliable after about 1950 (Karl and Steurer 1990; Jones and Henderson-Sellers 1992; Kaiser 1998). Dai et al. (1997b) examined the homogeneity in rain gauge records and removed the major discontinuities in the precipitation rec-

TABLE 1. The cross-correlation coefficients among daily mean cloud cover (cc), surface specific humidity (q), top 5-cm soil moisture content (sm), precipitation (P), wind speed (V), meridional wind (v), and the daily mean (T_a), minimum (T_{min}), maximum (T_{max}), and diurnal range (DTR) of surface air temperature from the FIFE site-average dataset. The numbers in boldface are statistically significant at ≤1% levels based on the random phase test (Ebisuzaki 1997). For a given correlation coefficient, its significance depends on the sample size (which varies from one variable to another) and the autocorrelation of the variables.

Variable	cc	q	sm	P	V	v	T_a	T_{min}	T_{max}	DTR
a, Summer, JJA										
cc	**1.00**	0.07	0.25	**0.34**	−0.16	**−0.30**	**−0.42**	−0.19	**−0.49**	**−0.52**
q	0.07	**1.00**	0.13	0.17	**0.22**	**0.34**	**0.65**	**0.80**	**0.52**	**−0.34**
sm	0.25	0.13	**1.00**	**0.26**	−0.17	−0.26	−0.36	−0.21	**−0.42**	**−0.35**
P	**0.34**	0.17	**0.26**	**1.00**	−0.10	−0.15	−0.13	−0.03	−0.14	**−0.19**
V	−0.16	**0.22**	−0.17	−0.10	**1.00**	**0.70**	**0.41**	**0.42**	**0.38**	−0.01
v	**−0.30**	**0.34**	−0.26	−0.15	**0.70**	**1.00**	**0.59**	**0.53**	**0.56**	0.13
T_a	**−0.42**	**0.65**	−0.36	−0.13	**0.41**	**0.59**	**1.00**	**0.92**	**0.95**	0.17
T_{min}	−0.19	**0.80**	−0.21	−0.03	**0.42**	**0.53**	**0.92**	**1.00**	**0.80**	−0.18
T_{max}	**−0.49**	**0.52**	**−0.42**	−0.14	**0.38**	**0.56**	**0.95**	**0.80**	**1.00**	**0.44**
DTR	**−0.52**	**−0.34**	**−0.35**	**−0.19**	−0.01	0.13	0.17	−0.18	**0.44**	**1.00**
b, Autumn, SON										
cc	**1.00**	0.16	0.11	**0.27**	0.09	−0.18	−0.09	0.10	**−0.28**	**−0.67**
q	0.16	**1.00**	0.02	**0.28**	0.13	**0.35**	**0.86**	**0.90**	**0.72**	−0.14
sm	0.11	0.02	**1.00**	0.11	−0.09	0.08	−0.18	−0.09	−0.21	−0.21
P	**0.27**	**0.28**	0.11	**1.00**	0.08	0.01	0.11	0.16	0.06	−0.15
V	0.09	0.13	−0.09	0.08	**1.00**	**0.40**	0.12	0.16	0.08	−0.11
v	−0.18	**0.35**	0.08	0.01	**0.40**	**1.00**	**0.43**	**0.37**	**0.47**	**0.26**
T_a	−0.09	**0.86**	−0.18	0.11	0.12	**0.43**	**1.00**	**0.96**	**0.94**	0.17
T_{min}	0.10	**0.90**	−0.09	0.16	0.16	**0.37**	**0.96**	**1.00**	**0.84**	−0.08
T_{max}	**−0.28**	**0.72**	−0.21	0.06	0.08	**0.47**	**0.94**	**0.84**	**1.00**	**0.47**
DTR	**−0.67**	−0.14	−0.21	−0.15	−0.11	**0.26**	0.17	−0.08	**0.47**	**1.00**

ords. The historical data of the changes in land use, dams, reservoirs, and levies are not readily available for most land areas and their effects on the streamflow data are not removed. As a cross-check, we will compare the decadal changes in these variables. Despite the errors, these observational datasets appear to be adequate and useful for decadal to long-term climate studies, especially for the last 4–5 decades.

3. Results

a. Daily relationships in FIFE site data

1) CORRELATIVE ANALYSIS

Trenberth (1991) showed that the anomalies in air temperature, humidity, and winds are intercorrelated over the storm track regions in the Southern Hemisphere on 2- to 8-day timescales. This suggests that synoptic systems may cause these variables to vary together. We calculated the cross-correlation coefficients among all the variables in the FIFE site dataset. Table 1 shows the cross correlation coefficients among the following variables: total cloud cover (cc), surface specific humidity (q), top 5-cm soil moisture content (sm), precipitation (P), surface wind speed (V), meridional wind (v), and the daily mean (T_a), minimum, maximum, and diurnal range of surface air temperature. As expected, southerly winds tend to be associated with higher specific humidity, T_{min}, T_{max}, and T_a, but not with DTR. The nighttime minimum temperature is strongly correlated ($r \geq 0.8$) with surface humidity, mainly because the downward radiation is highly correlated with the humidity (Table 2). On the other hand, the daytime maximum temperature correlates with not only the humidity, but also cloud cover, and soil moisture during summer. The JJA and SON T_{min} has little correlation with cloud cover, probably due to the fact that clouds reflect the sunlight, which reduces afternoon temperatures and thus the subsequent T_{min}, while they also enhance downward longwave radiation, which increases T_{min}. Except for V versus v, the correlations among the variables used in Fig. 1 are low (≤0.35) and often statistically insignificant. This suggests that most of the variations of cc, q, sm, P, and V are not correlated with each other on the daily timescale at the FIFE site.

Table 2 shows the correlations between the surface radiative and heat fluxes and cloud cover, surface moisture and other state variables at the surface. As expected, the surface downward solar radiation is negatively correlated with cloud cover. Although the cc–SolDn correlation is higher when daytime (e.g., 900–1500 LST) cloud cover is used ($r = -0.78$ for JJA and -0.65 for SON), it is still far from perfect, mainly because the observed cloud cover is for the whole sky and only part of it is between the sun and the observing station, which actually blocks the sunlight. This is also true for the cc–DTR correlations (i.e., only part of the observed cc blocks sunlight and thus affects T_{max} and DTR). The correlations between SolDn and the surface temperatures suggest that solar radiation increases daytime T_{max}

TABLE 2. The correlation coefficients between daily mean surface energy fluxes [of solar downward radiation (SolDn), longwave downward (LWDn) and upward (LWUp) radiation, latent (LH) and sensible (SH) heat, and the downward heat into the ground (*G*)] and the variables of Table 1 from the FIFE site average dataset and the low (cl) and high (ch) cloud cover from a nearby weather station (39.05°N, 96.77°W). The numbers in boldface are statistically significant at ≤1% levels based on the random phase test (Ebisuzaki 1997).

Variable	cc	cl	ch	q	sm	P	V	v	T_a	$T_{\min}$	$T_{\max}$	DTR
a, Summer, JJA												
SolDn	**−0.65**	**−0.53**	**−0.57**	−0.16	−0.18	**−0.32**	0.11	**0.21**	**0.32**	0.08	**0.40**	**0.54**
LWDn	0.23	**0.32**	0.15	**0.86**	−0.14	**0.28**	0.25	**0.32**	**0.62**	**0.79**	**0.52**	**−0.28**
LWUp	**−0.45**	−0.28	**−0.46**	**0.58**	−0.48	−0.15	0.43	**0.58**	**0.98**	**0.90**	**0.93**	0.24
LH	**−0.49**	**−0.39**	**−0.36**	0.00	0.09	**−0.23**	**0.22**	**0.27**	**0.28**	0.13	**0.32**	**0.33**
SH	−0.20	−0.09	**−0.32**	−0.22	**−0.33**	−0.11	−0.20	−0.20	−0.05	−0.20	0.02	**0.34**
G	**−0.43**	**−0.28**	**−0.35**	**0.29**	−0.25	**−0.21**	**0.25**	**0.45**	**0.60**	**0.48**	**0.59**	**0.22**
b, Autumn, SON												
SolDn	**−0.53**	**−0.37**	**−0.46**	0.28	−0.34	**−0.21**	−0.11	0.08	**0.50**	**0.35**	**0.60**	**0.53**
LWDn	**0.38**	**0.31**	**0.29**	**0.87**	0.08	**0.30**	0.13	**0.27**	**0.81**	**0.89**	**0.63**	**−0.27**
LWUp	0.07	0.01	−0.04	**0.90**	0.59	−0.02	0.13	**0.48**	**0.97**	**0.96**	**0.85**	−0.18
LH	−0.26	−0.05	−0.32	0.44	**0.65**	−0.09	−0.10	0.17	0.52	0.44	**0.54**	0.14
SH	−0.31	−0.05	−0.23	−0.47	−0.39	−0.06	−0.06	**−0.51**	**−0.43**	**−0.53**	−0.29	**0.35**
G	0.12	−0.07	0.09	**0.65**	−0.01	−0.08	0.23	**0.48**	**0.79**	**0.75**	**0.74**	−0.03

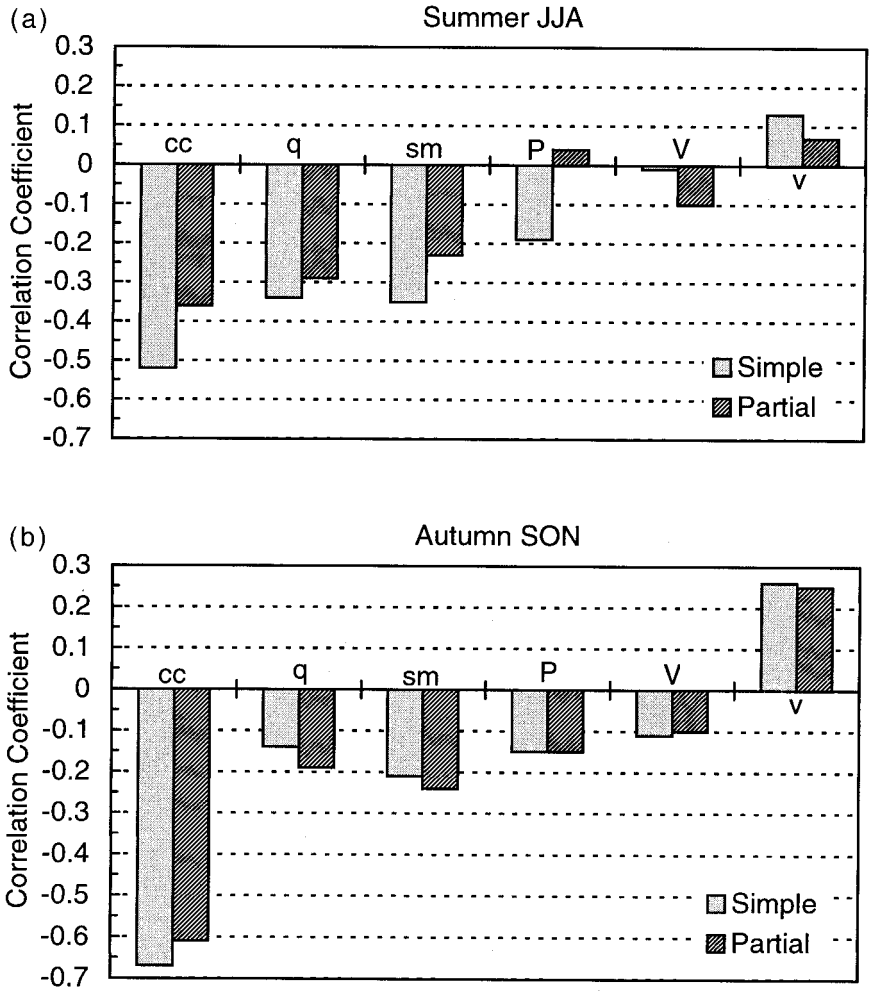

FIG. 1. Simple and partial correlation coefficients between daily DTR and total cloud cover (cc), surface humidity (*q*), top 5-cm soil moisture content (sm), precipitation (*P*), surface wind speed (*V*), and meridional wind (v) during summer and autumn at the FIFE site. Correlation coefficients larger than about 0.20 are statistically significant at a 1% level based on the random phase test (Ebisuzaki 1997).

more than that for nighttime T_{min} (negligible effect on JJA T_{min}, resulting in increased DTR. Partial correlations suggest that the SolDn–P correlation results mainly from the P–cc correlation, because physically precipitation falls from clouds that block the Sun.

The surface downward longwave radiation is strongly correlated with surface humidity and temperature, and not very sensitive to total, low, or high cloud amounts at the FIFE site during JJA and SON (Table 2). This is consistent with the notion that surface downward longwave radiation is most sensitive to lower atmospheric water vapor and temperature and less sensitive to cloud cover in the low latitudes and the midlatitudes during warm seasons (Fung et al. 1984; Zhang et al. 1995), presumably because there is sufficient amount of moisture in the air below clouds to decouple the surface temperature and clouds' downward longwave radiation. While higher LWDn is associated with both higher T_{max} and T_{min}, the T_{min} seems to depend more on LWDn than T_{max}, resulting in negative (although relatively low) DTR–LWDn correlations. The upward longwave radiation correlates strongly with surface air temperature and humidity and has little association with DTR (Table 2).

The surface latent heat flux depends strongly on SolDn ($r = 0.80$ for JJA and 0.53 for SON), which determines the energy available for evaporation, and on soil moisture in autumn. It is a surprise that LH is not correlated with sm in summer (Table 2). However, we will show that soil moisture does affect latent heat release in summer during the relatively clear-sky days. The surface sensible heat flux correlates significantly with T_a and T_{min} and meridional winds in autumn, but insignificantly with any of the variables except sm and DTR in JJA. The soil heat flux correlates mostly with surface air temperatures (Table 2).

Based on the above simple correlations and some physical consideration (e.g., wind speed may affect surface sensible and latent heat fluxes and thus surface temperatures), we linearly regressed daily DTR on the following variables: total cloud cover, surface specific humidity, top 5-cm soil moisture content, precipitation, surface wind speed, and meridional wind; and then computed the partial correlation coefficients based on this model (but skipping one variable each time). The inclusion of meridional wind is designed to detect the effects of advection of warm and cold air masses on DTR.

Figure 1 shows the simple and partial correlation coefficients between daily DTR and the above variables. It can be seen that among all these variables, clouds account for the largest amount of the DTR variance, especially in autumn. Soil moisture is negatively correlated with DTR in both summer and autumn, even after the effects of all the other variables are removed. This suggests that soil moisture is an important modulator of DTR whose effect on DTR cannot be accounted for by changes in clouds, surface humidity, precipitation, and winds. This is physically consistent with the idea that soil moisture provides moisture for evaporation that limits T_{max}. Surface humidity negatively correlates with DTR in summer, but the correlations are insignificant in autumn. Daily precipitation has very little correlation with DTR, suggesting that the direct effect (such as evaporative cooling) of precipitation on DTR is small, which is expected given the nocturnal maximum of rainfall at the FIFE site (Dai et al. 1999). However, when averaged over months or seasons and over large areas, precipitation can strongly correlate with DTR [cf. Fig. 12, also see Plantico and Karl (1990) and Dai et al. (1997a)]. This is expected because averaged over time precipitation is correlated with cloudiness (Dai et al. 1997b) and increases soil moisture.

Figure 1 also shows that wind speed is not correlated with DTR at the FIFE site, implying that the effects of wind on DTR through latent and sensible heat fluxes are likely to be small, mainly because their effect on surface temperatures has little diurnal variation. Meridional winds are positively correlated with DTR (i.e., southerly winds are associated with higher DTR) in autumn but not in summer, suggesting that the effect of advection of warm and cold air masses on DTR is negligible in summer while it may be significant in autumn and other seasons when advection is more prominent.

The relatively weak negative correlation between DTR and humidity may appear to be inconsistent with our daily experience. For example, the DTR over the Rocky Mountains is much larger than that in Florida, and one may attribute this to the large difference in atmospheric precipitable water over the two regions. However, further examination reveals that over the Rockies nighttime temperatures are lower because of the smaller downward surface longwave radiation that occurs at much higher altitudes (and thus lower temperatures). Thus, a large part of the DTR difference between the Rockies and Florida is due to the large difference in the equivalent altitude or temperature of downward surface longwave radiation. Tables 1 and 2 show that through its downward longwave radiation humidity increases both T_{min} and T_{max}, which makes it inefficient in damping DTR. In the following, we will present more evidence of the weak DTR–humidity association.

2) COMPOSITE ANALYSIS

Figure 2 shows the diurnal cycles T_a, total cloud cover q, the direction of the average winds, SH and LH fluxes, and SolDn and LWDn fluxes during summer in case 1. As expected, the southerly winds are associated with higher T_a and q. The surface downward longwave radiation is also ($\sim$30 W m^{-2}) higher when the winds come from the south. Despite the large T_a difference, the mean DTR of the days with southerly and northerly winds differs only slightly. The sensible and latent heat

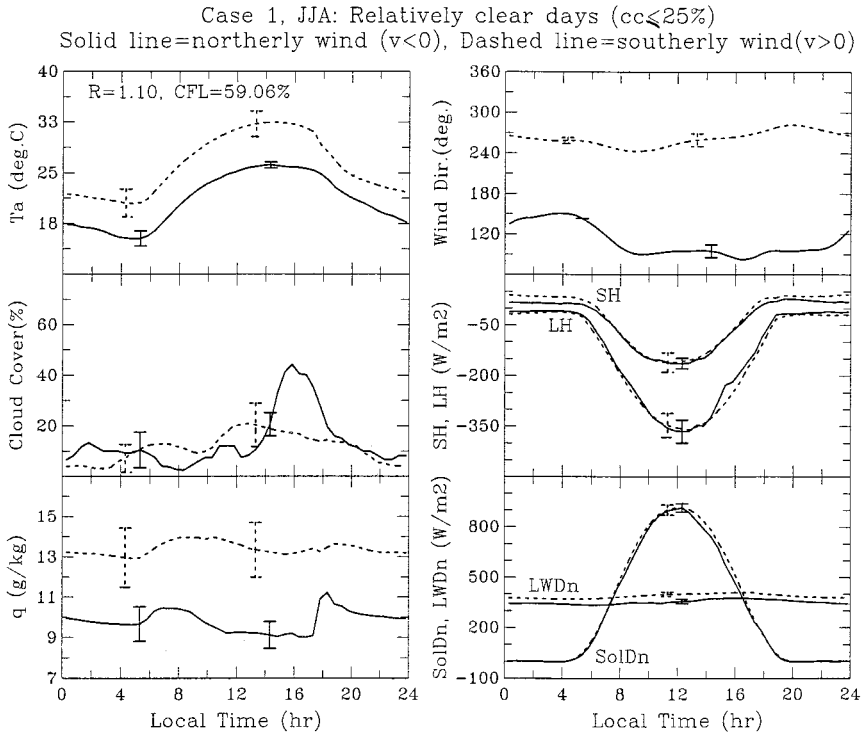

FIG. 2. Mean diurnal cycles of surface air temperature (T_a), cloud cover, surface specific humidity (q), surface wind direction (90° for winds from the north, 180° for winds from the west, and 270° for winds from the south), SH and LH heat fluxes (W m^{-2}), and SolDn and LW Dn downward radiation (W m^{-2}) for days with northerly (solid line) and southerly (dashed line) winds in case 1 during summer (JJA). The error bars represent the one-standard deviation range. Also shown are the dashed line to solid line ratio (R) of the diurnal T_a range and the confidence level for R being statistically different from 1.0 based on Student's t-test.

fluxes, which depend on the temperature and humidity gradients at the surface, are similar.

Figure 3 shows the diurnal cycles in case 2 during summer. It can be seen that the much higher cloud cover during the cloudy days (dashed line) reduces middle-day surface solar radiation by about 220 W m^{-2} compared with the clear days. This large reduction of solar radiation results in a much slower rise of daytime temperature from its early morning minimum. On the other hand, the nighttime temperature in the cloudy days is only slightly lower than that in the clear days, mainly because the downward longwave radiation, which largely controls nighttime temperatures, differs only slightly between the cloudy and clear days. This further suggests that clouds are not a dominant factor for surface downward longwave radiation. The predominant winds come from the south for both clear and cloudy days. Associated with the more rapid rise of the daytime temperature, the latent and sensible heat releases to the air tend to be higher in the clear days (while soil moisture is similar). It should be pointed out that the sensible and latent heat fluxes should depend more on the change rate of T_a than T_a itself because a rapid change of T_a can induce vertical gradients in temperature and humidity and thus affect sensible and latent heat fluxes. Also, because of their dependence on the change rate of T_a, the sensible and latent heat fluxes are usually passive and negative feedback terms rather than driving force for T_a like the radiative fluxes.

Figure 4 shows that LW Dn is about 80 W m^{-2} higher and T_a is about 8°C warmer in the high q days than in the low q days. While the temperatures in the lower atmosphere are likely to be higher during the higher q days (associated with the warmer surface T_a) and thus contribute to the enhanced LW Dn the higher humidity in the lower atmosphere in the high q days should also contribute to the enhanced LW Dn, given the large sensitivity of LW Dn to atmospheric water vapor (Zhang et al. 1995). In any case, the enhanced LW Dn increases both $T_{\min}$ and $T_{\max}$, resulting in a relatively small DTR reduction compared with the low q days. Both cloud cover and winds (from the south) are comparable for the low and high q days. Despite the large T_a difference, the sensible and latent heat fluxes are comparable in the low and high humidity days, consistent with the comparable change rates of T_a. While the model results of Stenchikov and Robock (1995) are qualitatively consistent with the mean T_a difference, Fig. 4 does not show

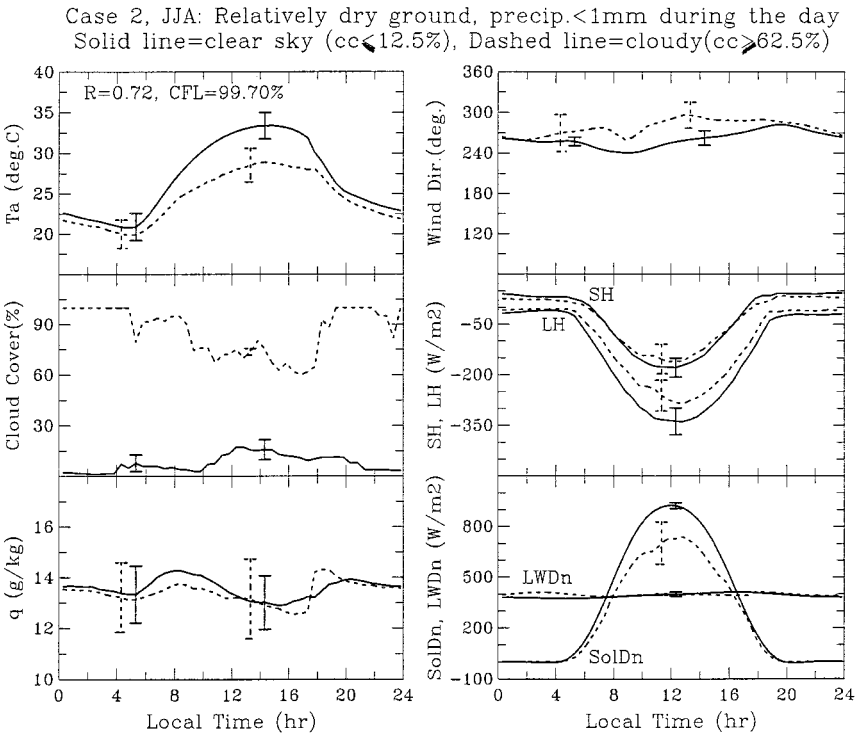

FIG. 3. Mean diurnal cycles, as in Fig. 2 but for the clear (solid line) vs cloudy (dashed line) days of case 2.

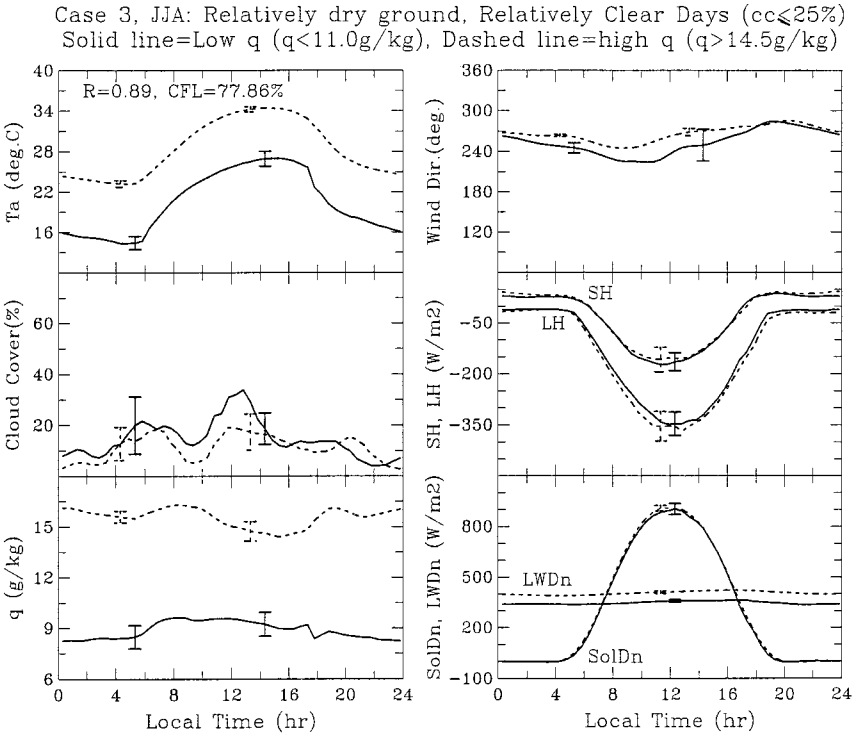

FIG. 4. Mean diurnal cycles, as in Fig. 2 but for the low (solid line) vs high (dashed line) surface humidity days of case 3.

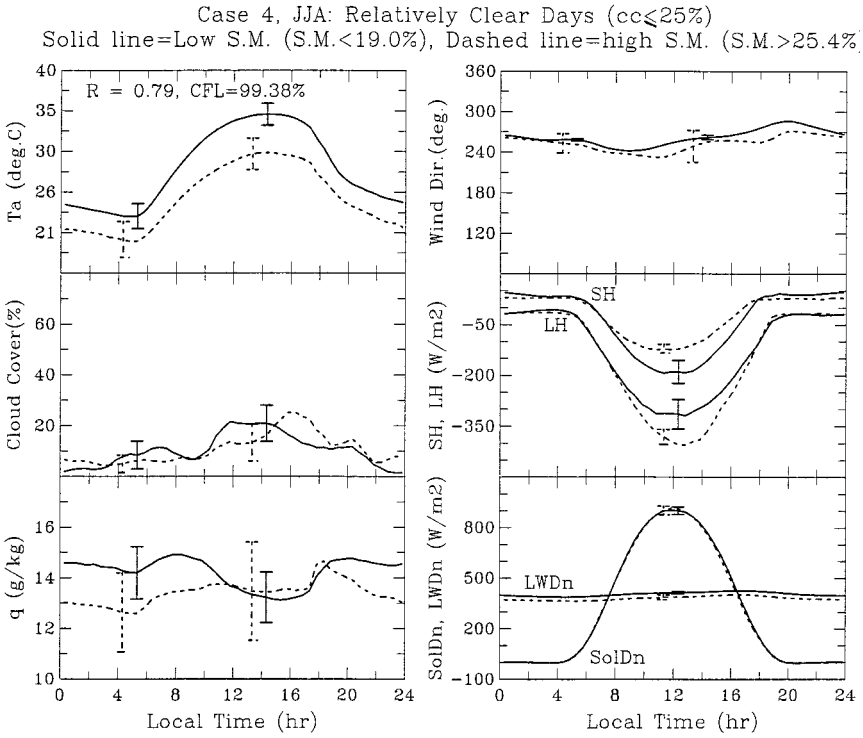

FIG. 5. Mean diurnal cycles, as in Fig. 2 but for the low (solid line) vs high (dashed line) soil moisture days of case 4.

significant differences in the downward solar radiation and DTR as suggested by their model.

Although latent heat flux is usually a feedback term for T_a, more surface soil moisture can increase the latent heat release and thus slow down the daytime increase of T_a (Fig. 5). Figure 5 shows that the effect of the ground dryness on LH exceeds that of the faster rise of daytime T_a, resulting in lower latent heat release, higher $T_{\max}$, and larger DTR during the relatively dry days. Associated with the more rapid rise of daytime T_a the sensible heat release is higher during the low soil moisture days, partly offsetting the reduced latent heat release.

Plots for case 5 (not shown) revealed that the differences in SH, LH, and DTR are insignificant between the calm and windy days in both summer and autumn, suggesting that the turbulence mixing in the calm days is not a limiting factor for sensible and latent heat releases at the FIFE site.

Figure 6 shows the combined effects of clouds, soil moisture, and others on DTR. This case differs from case 2 in that it also includes precipitating (and thus wet ground) days in the cloudy category. The cloud-induced reduction in surface solar radiation is more than 300 W m^{-2} from 1000 to 1400 local time, which greatly slows down the daytime rise of T_a and thus the sensible and latent heat releases in the cloudy days. Precipitation, which is often associated with optically thick clouds, increases surface soil moisture content and thus reduces time-averaged DTR (cf. Fig. 5). Therefore, even though we cannot separate the effects of precipitation on DTR from those of clouds and soil moisture, it is likely that precipitation also contributes to the 46% reduction in DTR during the cloudy and rainy days compared with the clear days.

The results for autumn are similar to those for summer, except that the reduction of DTR by clouds and soil moisture is much higher, mainly because the ground is generally drier in autumn, which results in lower latent heat releases to the air and thus more rapid rise of daytime T_a in the clear days. The combined effects of clouds, soil moisture, and water vapor result in an astonishing 62% reduction of DTR in the cloudy and rainy days compared with the clear days in autumn. The DTR reduction, as measured by the *dashed line to solid line* DTR ratio R in Figs. 2–6, is also much lower in autumn for case 2 with $R = 0.49$, but similar for the other cases compared with that of summer.

To summarize, the above correlative and composite results suggest that the diurnal cycle of surface air temperatures is driven by surface solar radiation. Because clouds can greatly modulate the solar radiation reaching the surface, they have the greatest damping effect on $T_{\max}$ and DTR. To a smaller extent, soil moisture also reduces DTR because it increases surface latent heat release and thus slows down the daytime rise of surface

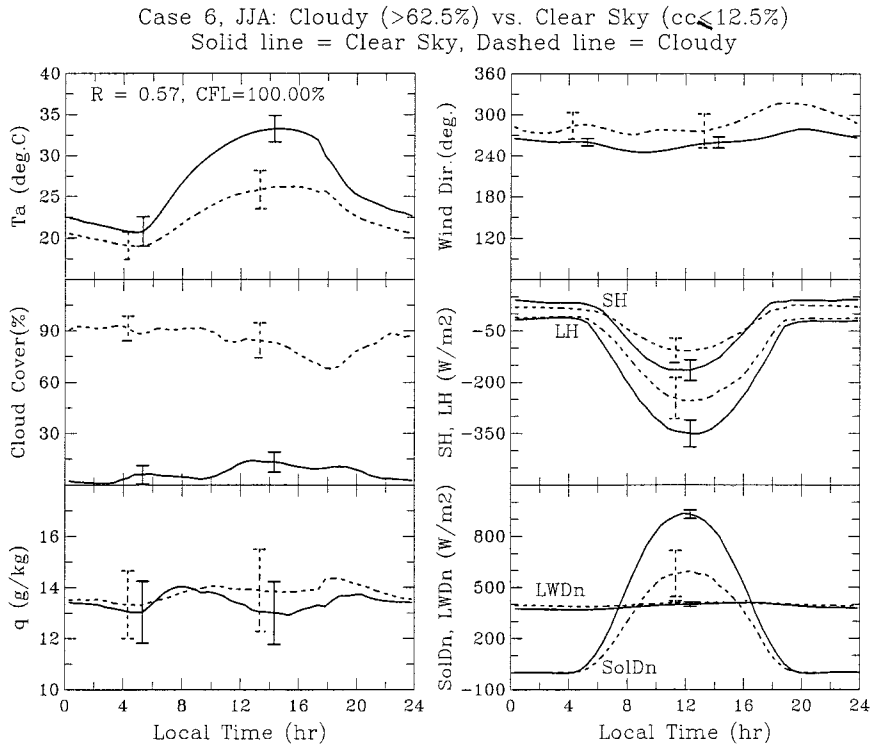

FIG. 6. Mean diurnal cycles, as in Fig. 2 but for the clear (solid line) vs cloudy and rainy (dashed line) days of case 6.

air temperatures. On the other hand, atmospheric water vapor increases both T_{max} and T_{min} and has a small effect on DTR, mainly because its greenhouse warming effect has little diurnal variation. Wind speed and the direct evaporative cooling of precipitation seem to have small effects on DTR.

b. Daily relationships in global station data

1) CORRELATIVE ANALYSIS

Figure 7 shows the simple correlation coefficients between daily DTR and total cloud cover (cc), surface specific humidity (q), and surface wind speed during northern winter (DJF) and summer (JJA) (maps for spring and autumn are comparable to that for JJA). It can be seen that total cloud cover is negatively correlated with DTR over most land areas. DTR-cc correlation is strongest (≤ -0.6) over western Europe, North America, eastern Asia, southern South America, and southern Africa. The correlation is low over northern mid- to high-latitudes in winter where solar radiation is weak. The cloud cover versus T_{min} or T_{max} (simple and partial) correlations revealed that T_{max} negatively correlates strongly with total cloud cover in JJA over most land areas and in DJF over areas south of about 30°N, while the cc–T_{min} correlation is generally weak ($r = -0.3 \sim 0.3$) except over the high latitudes in winter when sunshine length is short and the greenhouse warming effect of clouds exceeds their solar effect. This suggests that clouds damp DTR mainly by reflecting sunlight and thus reducing T_{max} whereas its net effect on T_{min} is relatively small during the warm seasons, especially over the low latitudes, which is consistent with the FIFE site results (Table 1). Further analyses revealed that low clouds have a stronger negative correlation with DTR and T_{max} than high and middle clouds, while the correlation of T_{min} with the three types of clouds is generally weak over low latitudes in all seasons and over high latitudes in summer. In winter over high latitudes, low clouds correlate positively with T_{min} more strongly than middle and high clouds, as one would expect. These results suggest that low clouds are more effective in damping DTR.

The correlation between DTR and surface humidity (Fig. 7) is low and insignificant over most land areas. Partial correlations suggest that most of the negative DTR-q correlations over the U. S. and a few other regions can be accounted for by clouds, and there are some positive DTR–q correlations ($r = 0.3 \sim 0.5$) over northern middle latitudes in spring and autumn. The maps of T_{min} versus q and T_{max} versus q correlation (strongest over northern middle to high latitudes with $r = 0.5 \sim 0.9$) and regression coefficients revealed similar magnitudes and spatial patterns. This suggests that the

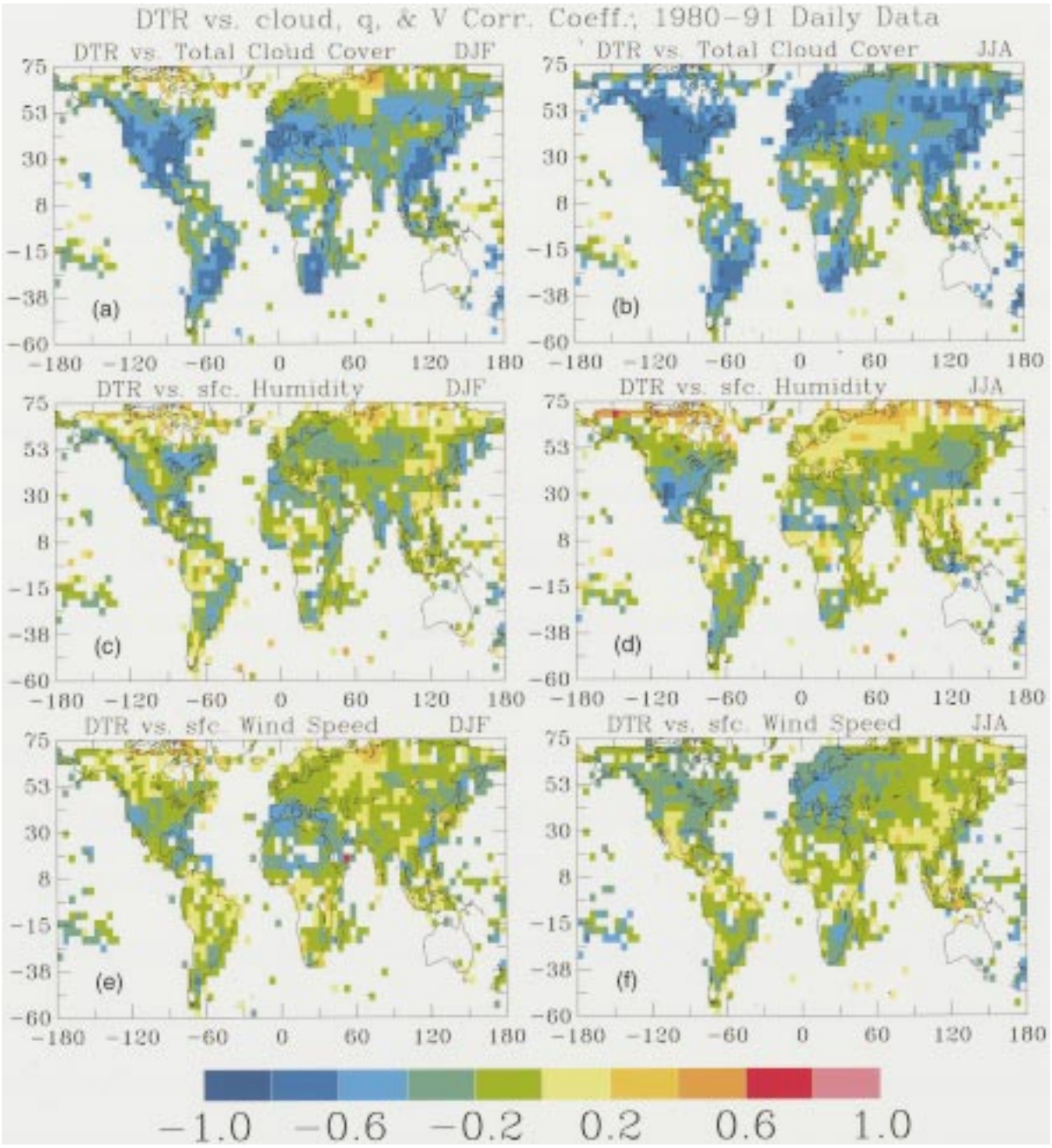

FIG. 7. Simple correlation coefficients between daily DTR and total cloud cover (a) and (b), surface humidity (c) and (d) and surface wind speed (e) and (f) for DJF (left column) and JJA (right column) calculated using the surface station observations from 1980 to 1991. Maps for spring and autumn are similar to those for JJA. Values above about 0.2 or below −0.2 are significant at ≤1% levels. White areas are without data (the same applies to all the color maps).

greenhouse warming effects of lower atmospheric water vapor on T_{min} and T_{max} are comparable, resulting in weak association between DTR and surface humidity. This is consistent with the FIFE data (cf. Fig. 4). The positive DTR–q correlations north of about 65° in summer likely result from the meridional advection of air masses with large humidity and DTR differences (cf. Fig. 8).

Figure 7 shows that correlation between DTR and surface wind speed is low and insignificant over most land areas. Most of the negative DTR–wind speed correlation over Europe and a few other regions results from the DTR–cloud correlation, as revealed by the partial correlations. These results suggest that the effects of winds on DTR through their influence on latent and sensible heat fluxes are likely to be small over most land areas.

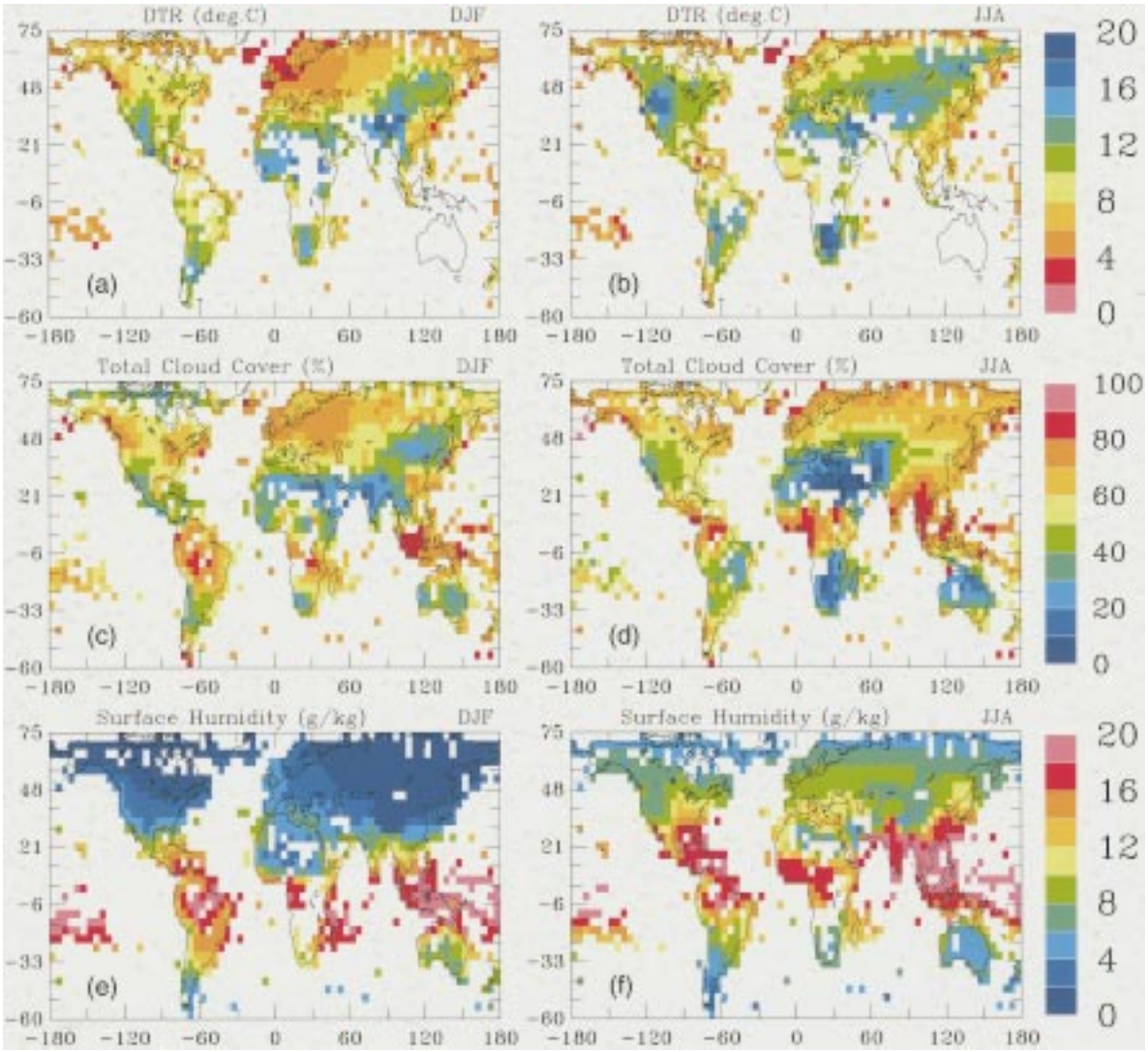

FIG. 8. Geographic distributions of the mean DJF and JJA DTR (°C) averaged over the 1980–91 period (top panels), together with the mean total cloud cover (middle panels) and surface specific humidity (bottom panels) for the same period. Maps for spring and autumn are comparable to JJA.

2) GEOGRAPHIC DISTRIBUTIONS

Figure 8 shows the geographic distribution of northern winter and summer DTR averaged over the 1980–91 period, together with the mean cloud cover and surface humidity distributions for the same period. It can be seen that DTR is about 4°–8°C over islands and coastal areas, and increases to 12°~20°C over inland and arid areas. Winter DTR is generally smaller than summer DTR over northern middle and high latitudes, while seasonal variations of DTR are small over islands, coastal areas, and the lower latitudes. In general, there is a good geographical, inverse correspondence between DTR and cloud cover over land (spatial correlation coefficient $r = -0.62$ for DJF and -0.60 for JJA, r is lower in low latitudes and higher in high latitudes): the regions with higher cloud cover generally have smaller DTR. For example, DTR is smaller in the eastern than in the southwestern United States while cloud cover is just the opposite. On the other hand, the correspondence between DTR and surface specific humidity is poor ($r = 0.06$ for DJF and -0.16 for JJA, much better with relative humidity which strongly correlates with cloud cover). We also computed precipitation frequency, which may be used as a proxy of ground wetness, and found that the geographic correspondence between DTR and precipitation frequency ($r = -0.57$ for DJF and -0.47 for JJA) and between cloud cover and precipitation frequency ($r = 0.33$ for DJF and 0.71 for JJA) is generally high. These results suggest that geographically DTR is largely determined by cloud cover, while atmospheric water vapor plays a secondary role, which is again consistent with the strong DTR–cc correlation

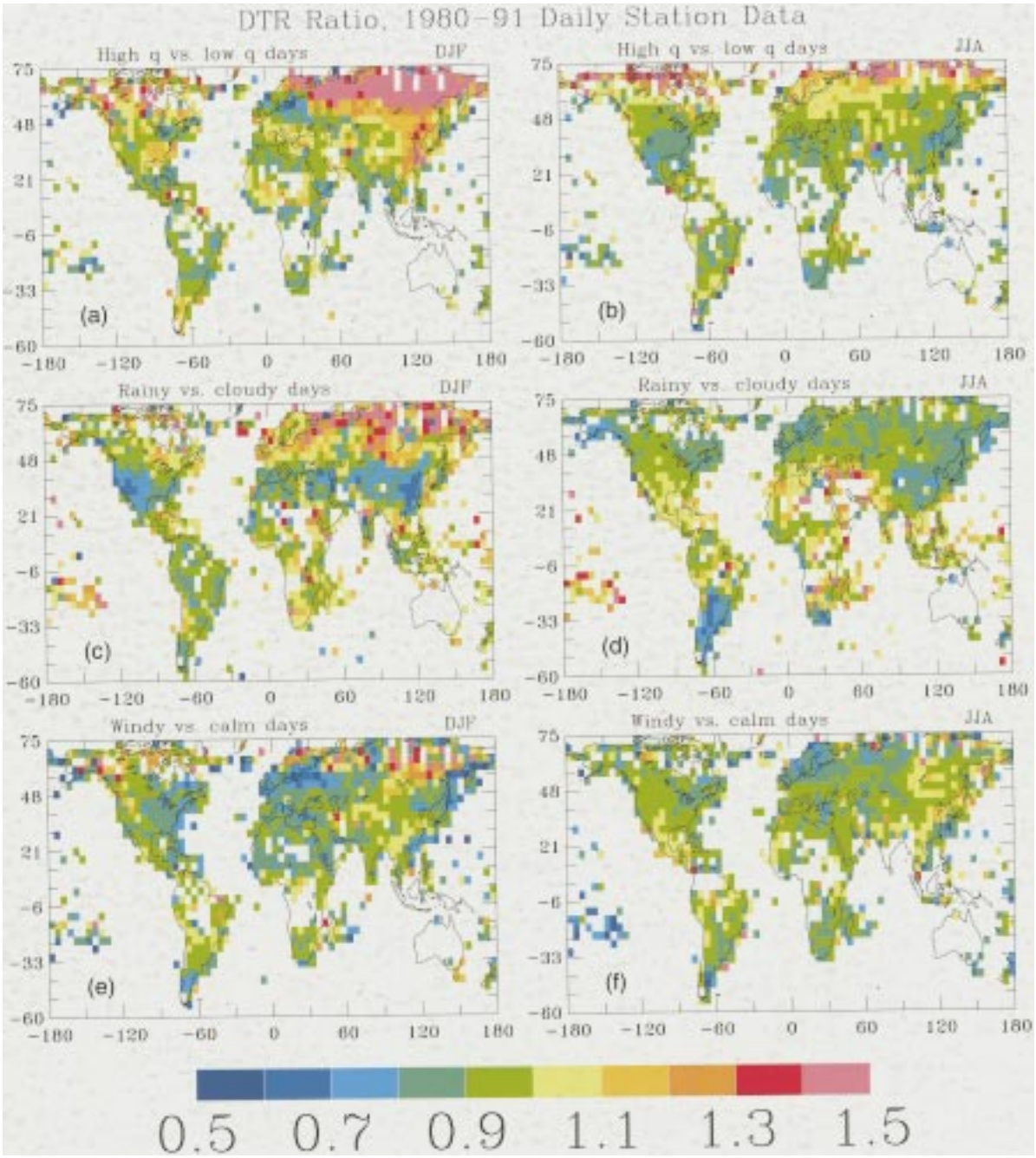

FIG. 9. Maps of the high to low humidity (a) and (b), rainy to cloudy days (c) and (d), and windy to calm days (e) and f) mean ratios of DTR for DJF and JJA seasons derived using the daily station data from 1980 to 1991. Values below about 0.8 or above 1.2 indicate that the DTRs are statistically different at ≤5% levels based on Student's t-test.

and the relatively weak DTR–*q* association in the FIFE data (cf. Figs. 1, 3, and 4).

3) COMPOSITE ANALYSIS

Figure 9 shows the DTR ratio between high and low surface humidity days with cc ≤25%, rainy and cloudy (with no precipitation) days, and windy and calm days with cc ≤25% for northern winter and summer (the DTR ratios for spring and autumn are also generally close to 1.0 over most land areas). Consistent with the weak correlations (Fig. 7), the DTR of the high humidity or windy days is only slightly lower than that of low humidity or calm days (and the differences are statis-

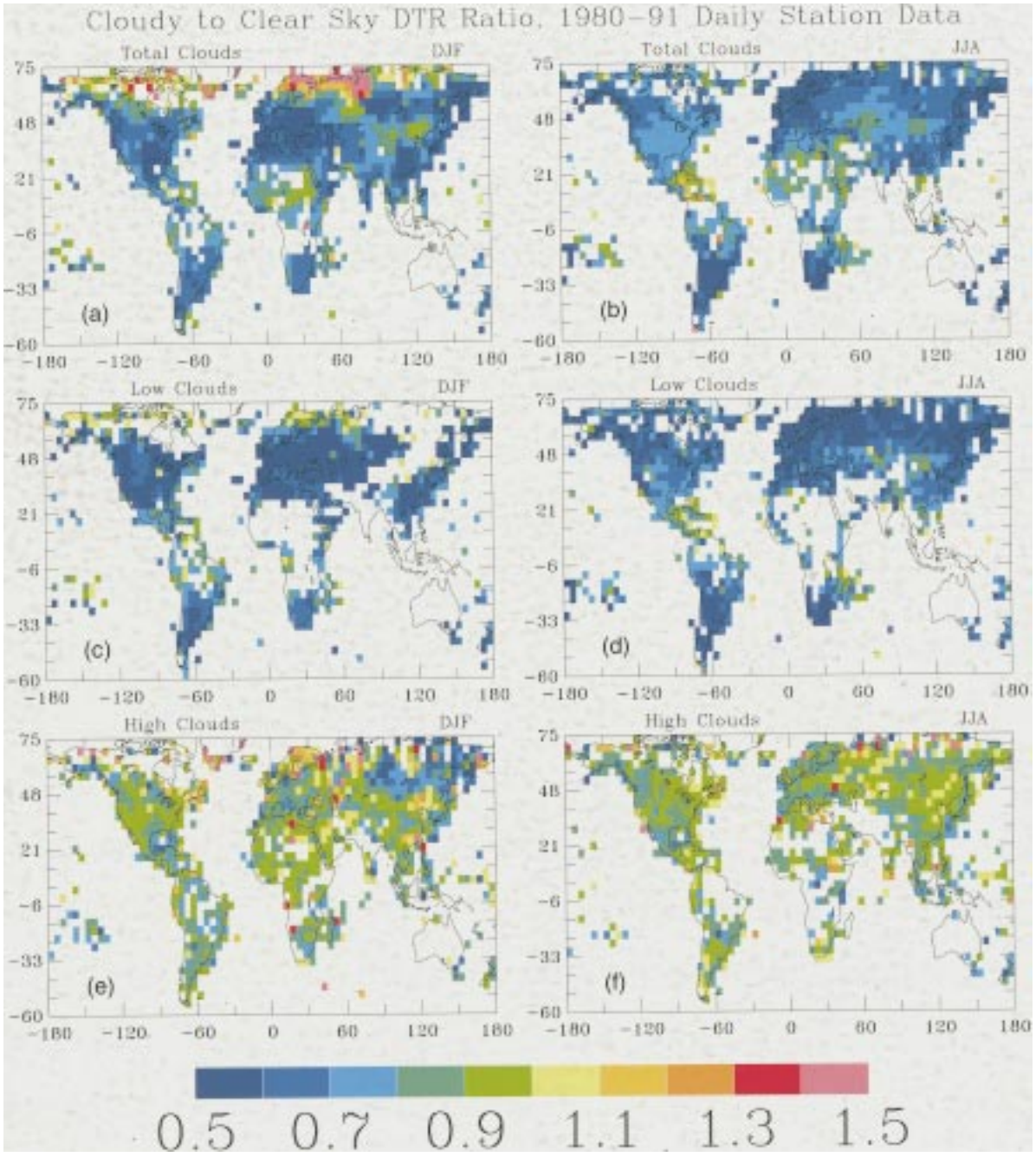

FIG. 10. Same as Fig. 9 but for cloudy (total cloud cover ≥5 oktas, including rainy days) to clear (cloud cover ≤1 okta) day ratio of DTR (a) and (b); mean ratio of DTR of days with low cloud cover ≥5 oktas, middle and high cloud cover ≤2 oktas, and no precipitation to DTR of clear days (c) and (d); and mean ratio of DTR of days with high cloud cover ≥5 oktas, low and middle cloud cover ≤2 oktas, and no precipitation to DTR of clear days (e) and (f).

tically insignificant) over most land areas. Over northern high latitudes such as Russia and northern Canada, where mean q is below 1 g kg^{-1} in winter (Fig. 8), DTR tends to be larger with higher surface humidity, especially in winter and autumn. Further examination of the station data revealed that winds on the low (high) humidity days often come from the north to northwest (west to southwest) over these high-latitude regions during winter. The northerly winds also bring in much ($>$10°C) colder air masses, which have a smaller DTR from the Arctic (cf. Fig. 8). Thus, a large portion of the DTR ratio between the high and low humidity days results from the advection of air masses with large DTR differences.

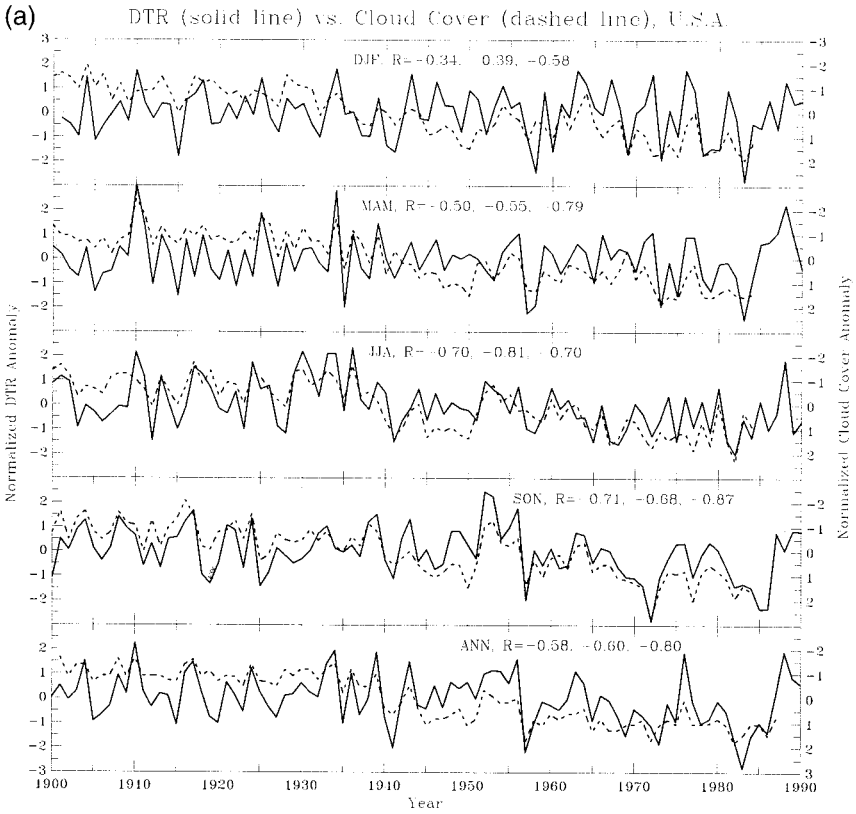

FIG. 11. Normalized (by standard deviation) seasonal and annual time series of DTR (solid line) and total cloud cover (dashed line) averaged over the (a) United States, (b) midlatitude (south of 60°N) Canada, (c) the former U.S.S.R., and (d) eastern (east of 100°E) China. Note the scale for cloud cover increases downward on the right side. Also shown are the correlation

Over many islands and western Europe, DTR tends to be lower in the windy days because strong maritime winds greatly reduce daytime T_{max} over these regions. Stronger winds may also reduce the stratification and increase the mixing in the lower atmosphere and thus reduce DTR, although this mechanism appears to have a small effect on DTR at the FIFE site and over most inland areas. Compared with cloudy days, DTR of rainy days is only slightly lower in summer over northern middle and high latitudes and southern South America, and in winter over the United States and China, suggesting that the direct effects (such as evaporative cooling) of precipitation on DTR are generally small, despite the fact that in summer precipitation occurs more often in the afternoon over many land areas (Dai et al. 1999). (However, the evaporative cooling associated with precipitation can reduce both T_{max} and T_{min} significantly.) In northern Eurasia, DTR is actually higher on rainy days compared with cloudy days, mainly because the rainy days are often associated with westerly or southwesterly winds, which bring in air masses with higher humidity and DTR.

Figure 10a and b shows the geographic distribution of the cloudy (including rainy) to clear day ratio of DTR for DJF and JJA. It can be seen that the DTR of cloudy and rainy days is generally lower (by as much as 50%) than that of clear days over most land areas, especially over Europe, North America (stronger reduction in spring and autumn than in summer), eastern Asia, southern South America, and southern Africa. When the rainy days are excluded, the DTR ratio is slightly higher, but still significantly below 1.0 and exhibits similar spatial patterns. One exception in Fig. 10 is over northern high latitudes in winter when sunshine is weak and short (and thus minimizing cloud's solar effects on T_{max}), where the DTR of cloudy and rainy days tends to be higher or similar to that of clear days. The maps of the cloudy to clear day DTR ratio for spring and autumn are very similar to that for JJA, except that the ratio is slightly smaller (i.e., larger reduction in cloudy days), especially over North America and in autumn. In general, the DTR reduction is largest in autumn over North America and Eurasia. This is expected because the ground is relatively dry in autumn in northern middle latitudes and thus there is limited latent heat release at the surface so that the daytime T_{max} depends more on cloud cover. The cloudy to clear day ratio of DTR is generally closer to 1.0 over the deserts and arid areas, mainly because the mean DTR is much larger over these regions (Fig. 8)

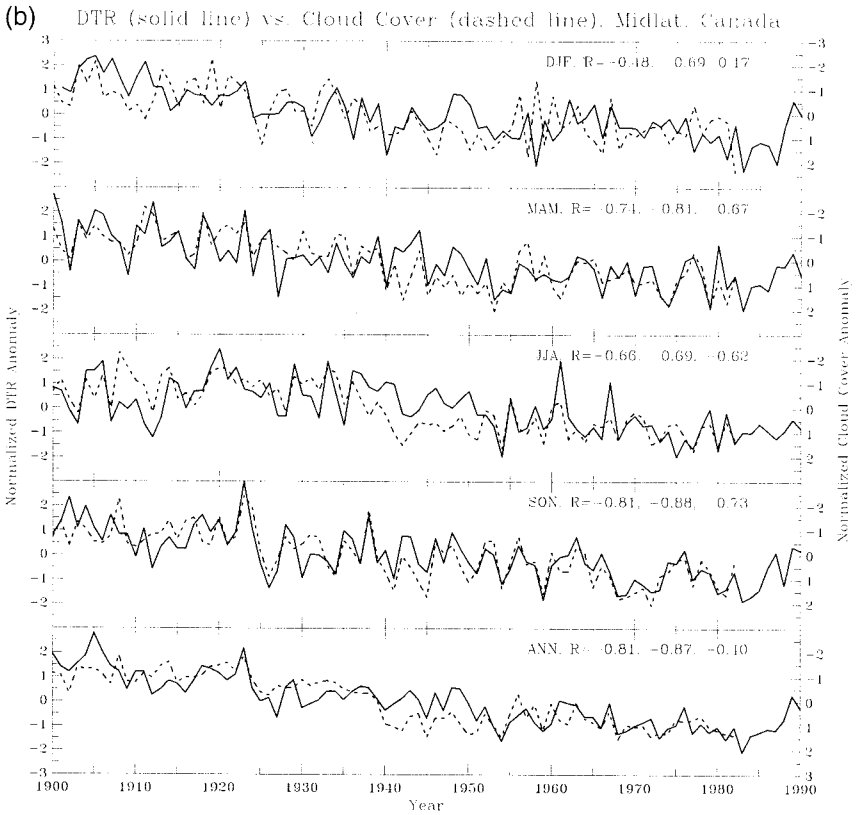

FIG. 11. (*Continued*) coefficients (R, abs(R) $> \sim 0.3$ is statistically significant) between the unfiltered DTR and cloud cover data, the filtered data with periods >7 yr and periods <7 yr, respectively, from the left to the right.

so that a given DTR ratio represents a larger absolute DTR change over the regions.

Figure 10 also shows the DTR ratio between cloudy (cc $\geq$ 5 oktas with no precipitation) days when clouds are mostly low (Fig. 10c and d) or high (Fig. 10e and f) clouds, and clear (cc $\leq$ 1 okta) days. It can be seen that compared with clear days DTR is generally 40%–50% lower when the sky is filled with $\geq$5 oktas of low clouds (of genera Sc, St, Cu, and Cb). On the other hand, DTR is only slightly ($\sim$10%) lower when the sky is filled with $\geq$5 oktas of high clouds (of genera Ci, Cc, and Cs) than that of clear days, suggesting that high clouds have only a small contribution to the DTR reduction by total clouds. It should be pointed out that the low clouds defined here include any nonprecipitating clouds with a low cloud base (<2 km above the ground) such as those deep convective clouds that may have high cloud tops. Although this definition of low clouds is not exactly the same as in Hansen et al. (1995), Fig. 10 is consistent with their model results, which suggest that for a given increase of cloud cover, low-level clouds cause the greatest decrease of DTR while high-level clouds cause a smaller decrease of DTR over land. This is expected because low clouds not only have larger solar albedo in general and thus reflect more sunlight and reduce T_{max} more efficiently than higher clouds, but also have lower cloud bases so that they can increase nighttime T_{min} efficiently through downward longwave radiation (however, the net effects of low or higher clouds on T_{min} tend to be small over low latitudes and in the summer high latitudes). The DTR ratios are consistent with correlative relationships discussed above (cf. Fig. 7).

The results from the analysis of the global station data suggests that the conclusions based on the FIFE data are valid over most land areas. In addition, clouds with low bases are found most effective in damping T_{max} and DTR mainly because they are often optically thick, while middle- and high-level clouds have only moderate damping effects on DTR. The damping effects of clouds on DTR are largest in warm and dry seasons when latent heat release is limited by the soil moisture content, and smallest in the winter high latitudes where sunshine is largely absent. In general, the net effect of clouds on T_{min} is small, except in the winter high latitudes where the greenhouse effect of clouds exceeds their solar cooling effect.

c. Relationships on multiyear to decadal timescales

Dai et al. (1997a) find that regionally averaged annual DTR is strongly correlated with cloud cover and pre-

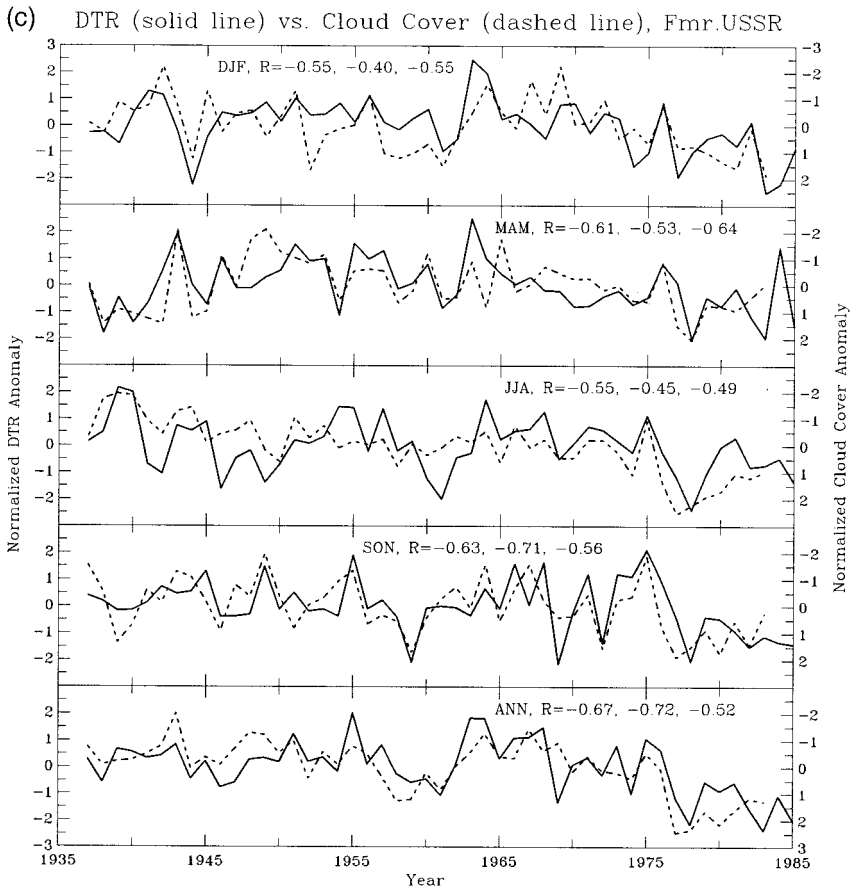

FIG. 11. (*Continued*)

cipitation on multiyear to decadal timescales. Figure 11 shows the seasonal time series of DTR and cloud cover averaged (using area as weighting) over the United States, midlatitude Canada, former U.S.S.R., and eastern China. It can be seen that in general DTR and cloud cover (inversely) covary fairly closely on interannual to decadal timescales, especially in autumn and over the United States and midlatitude Canada. The higher SON and lower DJF correlations are consistent with the seasonal patterns seen in daily data. It is remarkable that the decreasing long-term trends in DTR match well the increasing trends in cloud cover over midlatitude Canada. Similar relationships were found between the time series of DTR and precipitation over the regions of Fig. 11 (not shown).

Some of the increases of cloud cover from the late 1930s to the 1940s over the United States result from changes in observing practice (Karl and Steurer 1990). Although there are no similar analyses for the Canadian cloud data, it is possible that the addition of more observations per day and the change from tenth to okta in the reporting method around the late 1940s could have contributed to the cloud cover increase from the 1940s to early 1950s over midlatitude Canada. To separate the questionable decadal changes from the interannual to multiyear variations, we filtered the cloud cover and DTR data and examined the correlation on multiyear and decadal timescales. We found that, except for the DJF over midlatitude Canada where the multiyear variations are insignificantly correlated, the DTR–cloud cover correlations are statistically significant and in many cases are comparable on decadal and interannual to multiyear timescales (Fig. 11). This suggests that while some of the decadal changes in the cloud cover records may have resulted from changes in observing practice, overall the decadal to long-term changes in the cloud cover and DTR records are negatively correlated, and generally consistent with the relationships on daily and interannual to multiyear timescales.

Figure 12 shows that there is also some correlation between DTR and streamflow over the United States, midlatitude Canada, southeastern Australia, and Europe. This is expected because streamflow is correlated with precipitation and soil moisture content (Dai et al. 1998). However, the explained DTR variance (Fig. 12) is accounted for primarily by cloud cover and precipitation, which are also correlated with each other (Dai et al. 1997b). The summer to winter differences of the DTR–precipitation correlation coefficients (Fig. 12) are significant at a 1% level for the United States and mid-

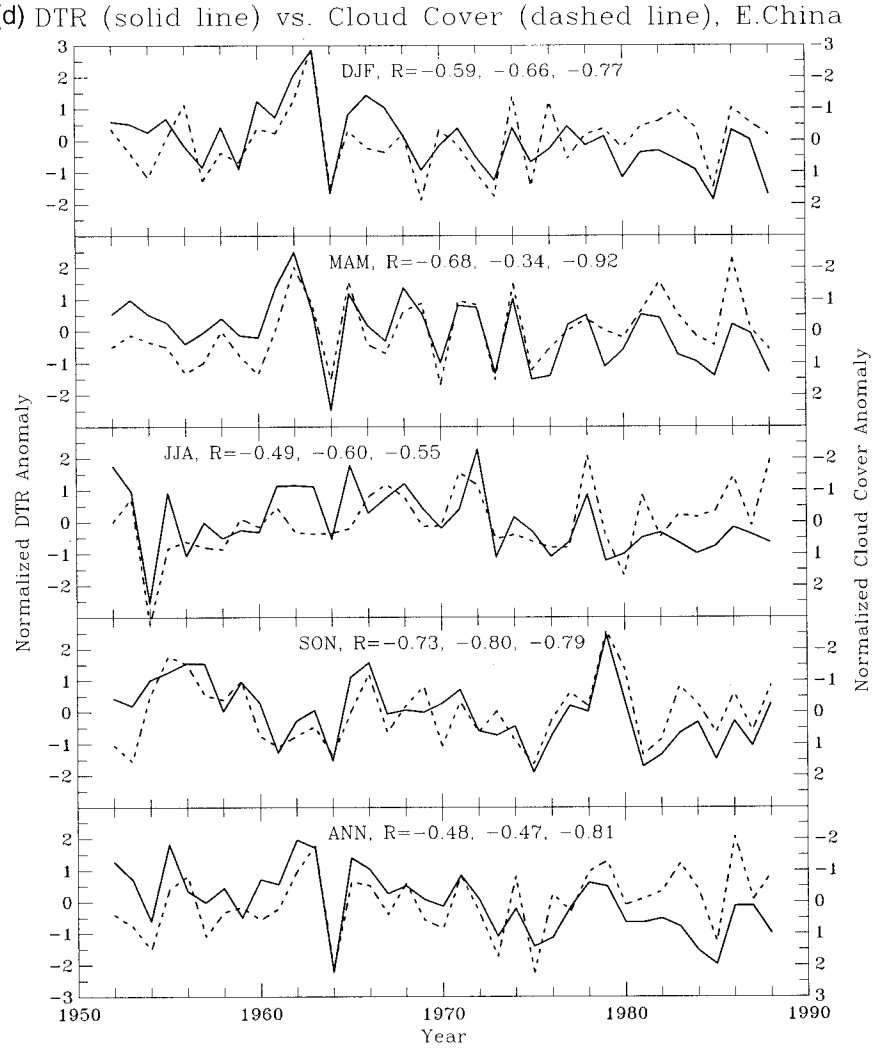

FIG. 11. (*Continued*)

latitude Canada and at a 5% level for Australia and Europe. The summer to winter differences of the DTR–cloud cover correlation coefficients are significant at a 1% level for the United States and midlatitude Canada. Figure 12 shows that up to 80% of the DTR variance can be explained by changes in cloud cover and precipitation over the United States, Australia, and midlatitude Canada. Combined with the above daily results, Fig. 12 strongly suggests that the DTR decreases over these regions during the last 4 to 5 decades (Fig. 11) (Easterling et al. 1997) result largely from the increases in cloud cover (Karl and Steurer 1990; Henderson-Sellers 1992) and precipitation (Bradley et al. 1987; Diaz et al. 1989; Dai et al. 1997b).

Over eastern China, DTR correlates better with cloud cover than with precipitation in all but the autumn season. Figure 11d shows that DTR follows cloud cover closely from 1952 until the late 1970s in eastern China. Thereafter, the cloud cover exhibited some moderate downward trends in spring and summer that the DTR failed to follow. In eastern China, air pollution is heaviest during winter and spring, and industrial sulfate emissions have increased exponentially since the early 1980s (Wang and Shi 1991). Because sulfate aerosols have a cooling effect on T_{max} (Karl et al. 1996), it is likely that the increasing industrial aerosols may have contributed to the DTR changes, especially in winter and spring, over eastern China during the last few decades.

Given the large reduction of DTR during cloudy and rainy days over Europe (Fig. 10), it is a surprise that the annual correlations and the explained DTR variance (Fig. 12) are relatively low over Europe. The relatively low DTR–cloud cover correlation over Europe results mainly from the interannual to multiyear variations (correlation coefficient $r = -0.28$ for variations with periods <7 yr and $r = -0.64$ with periods >7 yr). The DTR data over Europe are insufficient before 1950. The European cloud cover data were derived from only 58

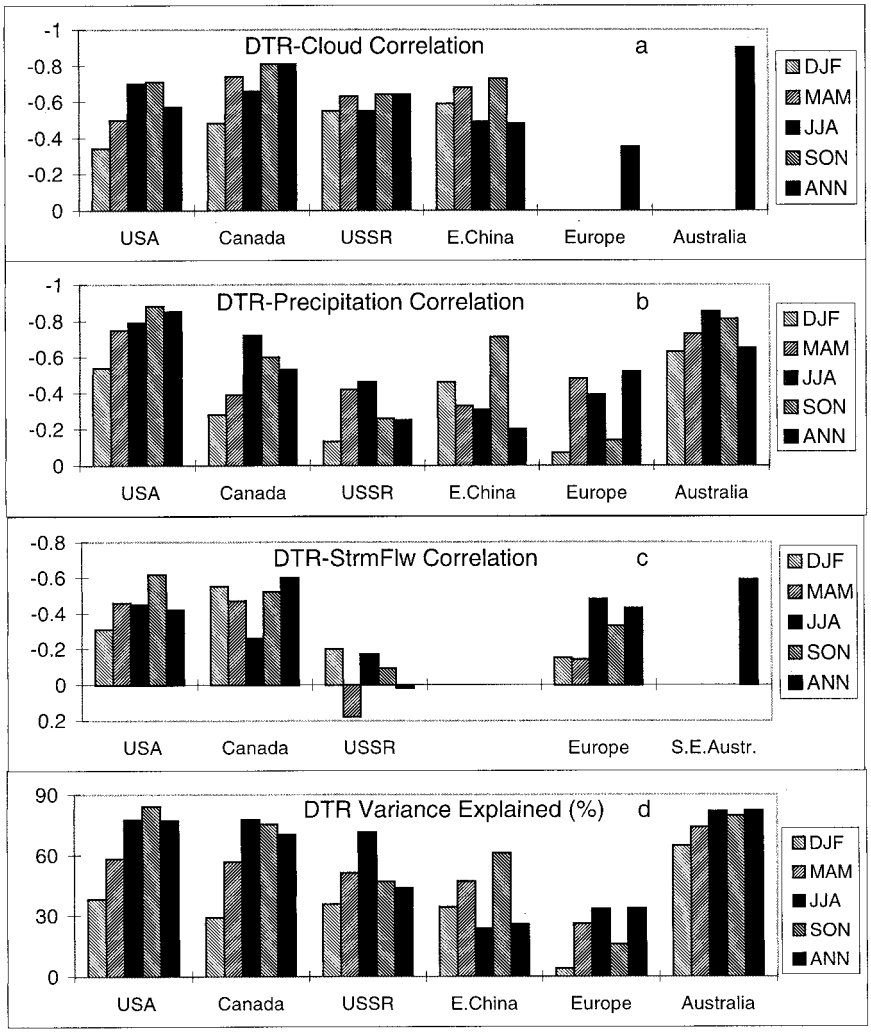

FIG. 12. Correlation coefficients of seasonal and annual DTR within the 1900–95 period with (a) total cloud cover, (b) precipitation, and (c) streamflow, and the percent variance (d) of DTR explained by cloud cover, precipitation, and streamflow (not available for eastern China and Australia) over the contiguous United States, midlatitude Canada, former U.S.S.R., eastern China, Europe, and Australia. Annual cloud cover was used for Europe and Australia in all seasonal calculations because the seasonal data were unavailable. The correlation coefficients above ~0.3 or below ~−0.3 are statistically significant.

stations located west of ~30°E (Henderson-Sellers 1992). While the European cloud cover data (for which we have only annual averages) correlate significantly with precipitation time series ($r = 0.62$ for the 1900–87 period) (Dai et al. 1997b), it is possible that the limited sampling is insufficient to capture the interannual variations (which are presumably more local than those with longer timescales) in the cloud cover. Also, over Europe precipitation anomalies (and thus cloudiness) associated with the North Atlantic Oscillation are out of phase in southern and northern Europe (Hurrell 1995; Dai et al. 1997), which makes the whole-Europe average of cloud cover less meaningful, especially on interannual to multiyear timescales (unfortunately, we do not have the station data of cloud cover over Europe to perform a more detail regional analysis). The industrial sulfur emission over Europe has been fairly stable (12–15 million tons of sulfur per year) since the 1950s (Dignon and Hameed 1989; Hameed and Dignon 1992) and is unlikely to have contributed to the DTR changes over Europe during this period.

Figure 13 compares the decadal variations and long-term trends during the last five decades in annual DTR, cloud cover, precipitation, and streamflow. It can be seen that both the decadal variations and trends are correlated among these variables over the United States and Australia while the decadal variations are less in phase over Europe and midlatitude Canada. The variables seem to be consistent with each other over the former U.S.S.R. although there are insufficient data for the latest decades.

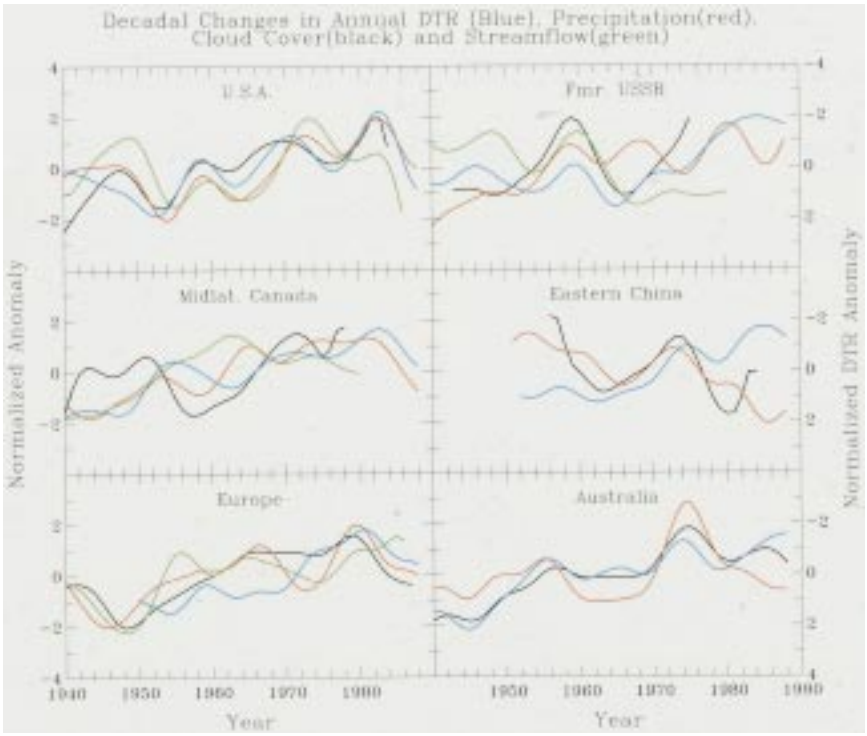

FIG. 13. Decadal changes of cloud cover (black line), precipitation (red line), streamflow (green line), and DTR (blue line) since 1940 over the same regions as in Fig. 12. Variations on timescales less than 10 yr are filtered out. Note that the DTR scale increases downward on the right side.

As pointed out above, DTR over eastern China departs from the trends in clouds and precipitation (which are correlated with each other) since the late 1970s. In general, Fig. 13 suggests that coinciding with the decreases in DTR, the hydrologic cycle has intensified during the last four to five decades over the United States, Australia, Europe, midlatitude Canada, and former U.S.S.R. The decreasing trends in cloud cover (Kaiser 1998) and precipitation over eastern China are one exception and need further investigation.

4. Summary and conclusions

Our results are limited by the quality and the sample sizes of the data. For example, there are less than 10 days of data in some of the plots in Fig. 4 (cf. section 2) and the results of these plots may not be representative. The historic cloud cover data used here were derived from limited spatial sampling and contain inhomogeneities resulting from changes in observing practice, especially from the 1930s to the 1940s. The streamflow data also contain inhomogeneities due to the changes in land use, dams, reservoirs, and levies. Although the FIFE data suggest that wind direction and advection have small effects on DTR, it may be important at other locations. For example, over the northern high latitudes, advection of the arctic cold and dry air masses induces a smaller DTR, which contributes to the smaller DTR on low humidity days over the region. We were unable to account for the effect of advection in our global analysis. Other factors, especially those having large diurnal variations such as fogs and haze, could also affect DTR. The soil moisture data used here are very limited and more comprehensive analyses of its effects on DTR are needed. Besides soil moisture, changes in land cover (e.g., associated with deforestation and desertification) could also affect daytime evapotranspiration and thus T_{max} and DTR. For example, a climate model study (Bonan 1998, manuscript submitted to *Ecol. Appl.*), suggests that the conversion of forest to cropland in the eastern and central United States during the first half of the nineteenth century resulted in a general cooling and a reduction of DTR of 0.6°–1.0°C in summer and autumn.

Our analysis of the daily data from the FIFE site and the global weather stations shows that clouds, soil moisture, and precipitation can reduce the surface diurnal temperature range by over 50% compared with clear sky days, while atmospheric water vapor increases both the T_{min} and T_{max} and has small effects on DTR over most land areas except the northern high latitudes where DTR tends to be larger in high humidity days in winter and autumn. Changes in wind directions, such as those associated with the passing of synoptic systems, can greatly alter the daily mean temperature but generally do not affect DTR significantly at the FIFE site. Clouds,

which contribute most of the DTR reduction and largely determine the mean magnitudes of DTR over most regions, reduce DTR by sharply decreasing surface solar radiation and thus the daytime maximum temperature, while soil moisture increases surface latent heat releases and slows down the temperature rise during the day in warm seasons. However, surface sensible heat fluxes tend to offset a large part of the latent heat release anomalies and make soil moisture less effective in damping DTR. Precipitation affects DTR mostly by increasing the soil moisture content while its direct damping on DTR is relatively small. The nighttime minimum temperature is largely controlled by the greenhouse effect of lower atmospheric water vapor, while the daytime maximum temperature depends heavily on the surface solar heating, which is strongly affected by cloud cover, and the amount of it that is released into the air by sensible and latent heat, which depends on soil moisture content. Stronger winds tend to reduce DTR over islands, western Europe, and some other coastal areas, but have a small effect on DTR over most inland areas.

Correlations between the nighttime minimum temperature and total, low, middle, and high cloud amounts are weak in all seasons in low latitudes and in summer in high latitudes. This suggests that, except for the winter high latitudes where solar radiation is at a minimum, the nighttime greenhouse warming effects of clouds tend to balance their daytime solar cooling effects on afternoon temperatures, resulting in small net effects on the nighttime minimum temperature. This further suggests that clouds damp DTR mainly by reducing the daytime maximum temperature over most land areas while their downward longwave radiation contributes little to the DTR reduction mainly because it has a relatively small diurnal asymmetry. Our results are consistent with those of Power et al. (1998), who find that over Australia annual precipitation, which is highly correlated with cloud cover, negatively correlates with T_{max} but generally not with T_{min}.

Clouds with low bases are found to be most efficient in reducing the daytime maximum temperature and DTR. High and middle clouds have only moderate damping effects on DTR mainly because they are usually optically thinner than clouds with low bases.

The reduction of DTR by clouds is largest in warm and dry seasons (e.g., SON for many northern midlatitude regions such as the United States, southern Canada, and Europe) and smallest in the winter high latitudes where sunshine is largely absent. This is expected because during warm and dry seasons surface latent heat release is limited so that the daytime maximum temperature depends more on the solar heating and thus clouds.

Seasonal DTR of the twentieth century inversely covary fairly closely with cloud cover and precipitation on interannual to decadal and longer timescales over the United States, Australia, midlatitude Canada, and former U.S.S.R. Over eastern China, DTR (inversely) follows cloud cover and precipitation from 1952 to the late 1970s. Thereafter, there have been some decreasing trends in cloud cover and precipitation while DTR has decreased slightly over eastern China, suggesting that other forcings such as the increased industrial sulfate aerosols may have contributed to the recent DTR variations over eastern China. Clouds and precipitation can account for up to 80% of the variance of the annual mean historical DTR changes.

The historical records suggest that there have been increases in cloud cover and precipitation during the last 4–5 decades over the United States, midlatitude Canada, Europe, Australia, and former U.S.S.R. Streamflow has also increased over the United States, Canada, and Europe (and is not available over Australia and China). During the same period, DTR has decreased over all these regions. Given the strong damping effect of clouds on DTR, as shown by the daily data, the well-established worldwide DTR decreases during the last 4–5 decades (Karl et al. 1993; Easterling et al. 1997) are consistent with the reported increasing trends in cloud cover (Karl and Steurer 1990; Henderson-Sellers 1992) and precipitation (Bradley et al. 1987; Diaz et al. 1989; Dai et al. 1997b) over many land areas and support the notion that the hydrologic cycle has intensified during the last 4–5 decades.

As pointed out above, clouds and soil moisture reduce DTR largely by decreasing T_{max} rather than increasing T_{min}. Therefore, increases in clouds and precipitation will slow down upward trends in T_{max} and have relatively small effects on T_{min}, which is consistent with the observed asymmetric trends in T_{min} and T_{max} (Karl et al. 1993; Easterling et al. 1997). However, correlations between historical cloudiness and T_{max} or T_{min} are much lower than the DTR–cloud correlation. This is expected because other forcings such as the increased greenhouse gases greatly affect T_{min} and T_{max} while DTR is influenced largely by forcings that have a diurnal asymmetry.

While our analyses of the historical data complement earlier studies by Karl et al. (1993), Dai et al. (1997a), and others on the statistical relationships between DTR and cloudiness and precipitation, our results from the analyses of FIFE and station daily data provide new evidence of strong damping effects of clouds (especially those with low bases) on DTR. The FIFE data also suggest that land use changes could modulate DTR significantly through surface evapotranspiration. This aspect has not been considered in earlier similar studies and requires further investigation.

Acknowledgments. We thank Alan Betts for providing the FIFE dataset, Dale Kaiser for sharing his Chinese cloud data with us, Joel Norris for helpful discussions on synoptic weather reports of clouds, and Pasha Groisman for many helpful comments. A. Dai is supported by a NOAA Post-doctoral Program in Climate and Global Change fellowship, administered by the University Corporation for Atmospheric Research.

REFERENCES

Betts, A. K., and J. H. Ball, 1998: FIFE surface climate and site-average dataset: 1987–1989. *J. Atmos. Sci.,* **55,** 1091–1108.

Bradley, R. S., H. F. Diaz, J. K. Eischeid, P. D. Jones, P. M. Kelly, and C. M. Goodess, 1987: Precipitation fluctuation over Northern Hemisphere land areas since the mid-19th century. *Science,* **237,** 171–175.

Campbell, G. G., and T. H. Vonder Haar, 1997: Comparison of surface temperature minimum and maximum and satellite measured cloudiness and radiation budget. *J. Geophys. Res.,* **102,** 16 639–16 645.

Cao, H. X., J. F. B. Mitchell, and J. R. Lavery, 1992: Simulated diurnal range and variability of surface temperature in a global climate model for present and doubled CO_2 climates. *J. Climate,* **5,** 920–943.

Dai, A., A. D. Del Genio, and I. Fung, 1997a: Clouds, precipitation, and temperature range. *Nature,* **386,** 665–666.

——, I. Y. Fung, and A. D. Del Genio, 1997b: Surface observed global land precipitation variations during 1900–88. *J. Climate,* **10,** 2943–2962.

——, K. E. Trenberth, and T. R. Karl, 1998: Global variations in droughts and wet spells: 1900–1995. *Geophys. Res. Lett.,* **25,** 3367–3370.

——, F. Giorgi, and K. E. Trenberth, 1999: Observed and model simulated precipitation diurnal cycle over the contiguous United States. *J. Geophys. Res.,* **104,** 6377–6402.

Dessens, J., and A. Bücher, 1995: Changes in minimum and maximum temperatures at the Pic du Midi in relation with humidity and cloudiness. *Atmos. Res.,* **37,** 147–162.

Diaz, H. F., R. S. Bradley, and J. K. Eischeid, 1989: Precipitation fluctuations over global land areas since the late 1800's. *J. Geophys. Res.,* **94,** 1195–1210.

Dignon, J., and S. Hameed, 1989: Global emissions of nitrogen and sulfur oxides in fossil fuel combustion from 1860 to 1980. *J. Air Waste Manage. Assoc.,* **39,** 180–186.

Easterling, D. R., and Coauthors, 1997: Maximum and minimum temperature trends for the globe. *Science,* **277,** 364–367.

Ebisuzaki, W., 1997: A method to estimate the statistical significance of a correlation when the data are serially correlated. *J. Climate,* **10,** 2147–2153.

Fung, I. Y., D. E. Harrison, and A. A. Lacis, 1984: On the variability of the net longwave radiation at the ocean surface. *Rev. Geophys. Space Phys.,* **22,** 177–193.

Hahn, C. J., S. G. Warren, and J. London, 1996: Edited synoptic cloud reports from ships and land stations over the globe, 1982–1991. Tech. Rep. NDP-026B, Carbon Dioxide Information Analysis Center, Oak Ridge National Laboratory, TN, 45 pp. [Available from CDIAC, Oak Ridge National Laboratory, Oak Ridge, TN 37831.]

Hair, J. F., Jr., R. E. Anderson, and R. L. Tatham, 1987: *Multivariate Data Analysis.* 2d ed. Macmillan Publishing Company, 449 pp.

Hameed, S., and J. Dignon, 1992: Global emissions of nitrogen and sulfur oxides in fossil fuel combustion 1970–1986. *J. Air Waste Manage. Assoc.,* **42,** 159–163.

Hansen, J., M. Sato, and R. Ruedy, 1995: Long-term changes of the diurnal temperature cycle: Implications about mechanisms of global climate change. *Atmos. Res.,* **37,** 175–210.

Henderson-Sellers, A., 1989: North American total cloud amount variations this century. *Global Planet. Change,* **75,** 175–194.

——, 1992: Continental cloudiness changes this century. *Geo J.,* **27,** 255–262.

Horton, E. B., 1995: The geographical distribution of changes in maximum and minimum temperatures. *Atmos. Res.,* **37,** 101–117.

Houghton, J. T., L. G. Meira Filho, B. A. Callander, N. Harris, A. Kattenberg, and K. Maskell, Eds., 1996: *Climate Change 1995: The Science of Climate Change.* Cambridge University Press, 572 pp.

Hurrell, J. W., 1995: Decadal trends in the North Atlantic Oscillation: Regional temperatures and precipitation. *Science,* **269,** 676–679.

Jones, P. A., and A. Henderson-Sellers, 1992: Historical records of cloudiness and sunshine in Australia. *J. Climate,* **5,** 260–267.

Jones, P. D., 1995: Maximum and minimum temperature trends in Ireland, Italy, Thailand, Turkey, and Bangladesh. *Atmos. Res.,* **37,** 67–78.

Kaas, E., and P. Frich, 1995: Diurnal temperature range and cloud cover in the Nordic countries: Observed trends and estimates for the future. *Atmos. Res.,* **37,** 211–228.

Kaiser, D. P., 1998: Analysis of monthly mean cloud amount for China: 1951–1994. Preprints, *Ninth Symp. on Global Change Studies,* Phoenix, AZ, Amer. Meteor. Soc., 168–172.

Karl, T. R., and P. M. Steurer, 1990: Increased cloudiness in the United States during the first half of the twentieth century: Fact or fiction? *Geophys. Res. Lett.,* **17,** 1925–1928.

——, and Coauthors, 1993: Asymmetric trends of daily maximum and minimum temperature. *Bull. Amer. Meteor. Soc.,* **74,** 1007–1023.

——, R. W. Knight, G. Kukla, and J. Gavin, 1996: Evidence for radiative effects of anthropogenic sulfate aerosols in the observed climate record. *Aerosol Forcing of Climate,* R. Charlson and J. Heintzenberg, Eds., Wiley & Sons, 363–382.

Kukla, G., and T. R. Karl, 1993: Nighttime warming and the greenhouse effect. *Environ. Sci. Technol.,* **27,** 1468–1474.

Mitchell, J. F. B., R. A. Davis, W. J. Ingram, and C. A. Senior, 1995: On surface temperature, greenhouse gases, and aerosols: Models and observations. *J. Climate,* **8,** 2364–2386.

Peterson, T. C., and R. S. Vose, 1997: An overview of the Global Historical Climatology Network temperature data base. *Bull. Amer. Meteor. Soc.,* **78,** 2837–2849.

Plantico, M. S., and T. R. Karl, 1990: Is recent climate change across the United States related to rising levels of anthropogenic greenhouse gases? *J. Geophys. Res.,* **95,** 16 617–16 637.

Power, S., F. Tseitkin, S. Torok, B. Lavery, R. Dahni, and B. McAvaney, 1998: Australian temperature, Australian rainfall and the Southern Oscillation, 1910–1992: Coherent variability and recent changes. *Aust. Meteor. Mag.,* **47,** 85–101.

Stenchikov, G. L., and A. Robock, 1995: Diurnal asymmetry of climatic response to increased CO_2 and aerosols: Forcings and feedbacks. *J. Geophys. Res.,* **100,** 26 211–26 227.

Trenberth, K. E., 1991: Storm tracks in the Southern Hemisphere. *J. Atmos. Sci.,* **48,** 2159–2178.

Wang, W., and Q. Shi, 1991: Analysis of the formation of air pollution and acid rain in China. *Proc. Second IUAPPA Regional Conf. on Air Pollution,* Vol. 2, Seoul, Korea, Korea Air Pollution Research Association, 49–56.

Zhang, Y.-C., W. B. Rossow, and A. A. Lacis, 1995: Calculation of surface and top of atmosphere radiative fluxes from physical quantities based on ISCCP data sets. Part 1: Methods and sensitivity to input data uncertainties. *J. Geophys. Res.,* **100,** 1149–1165.